On Large-Cohort Training for Federated Learning

Zachary Charles [1] **Zachary Garrett** [1] **Zhouyuan Huo** [1] **Sergei Shmulyian** [1] **Virginia Smith** [2]

Abstract

Federated learning methods typically learn a model by iteratively sampling updates from a population of clients. In this work, we explore how the number of clients sampled (the *cohort size*) impacts the quality of the learned model and the training dynamics. Our work poses three fundamental questions: First, what challenges arise when scaling federated learning to larger cohorts? Second, what parallels exist between cohort sizes in federated learning and batch sizes in centralized learning? Last, how can we design better large-cohort training methods? We give partial answers to these questions based on extensive empirical evaluation, highlighting challenges that arise from the use of larger cohorts. While some of these are analogs of large-batch training challenges, others are unique to federated learning.

1. Introduction

Federated learning (FL) (McMahan et al., 2017) considers learning a model from clients without directly sharing data. In this work we focus on *cross-device* FL, in which the aim is to learn across a large population of edge devices (Kairouz et al., 2021, Table 1). A distinguishing characteristic of cross-device FL is *partial client participation*: Due to systems constraints, the server typically only communicates with a small subset of clients in each round[1]. For example, in the popular `FedAvg` algorithm (McMahan et al., 2017), at each communication round the server broadcasts its current model to a subset of available clients (referred to as a *cohort*), who use the model to initialize local optimization and send their model updates back to the server.

[1]Google [2]Carnegie Mellon University. Correspondence to: Zachary Charles <zachcharles@google.com>.

This work was presented at the International Workshop on Federated Learning for User Privacy and Data Confidentiality in Conjunction with ICML 2021 (FL-ICML'21). This workshop does not have official proceedings and this paper is non-archival.

[1]In contrast, *cross-silo* settings often have a small set of clients, most of which participate in each round (Kairouz et al., 2021).

Intuitively, larger cohort sizes have the potential to improve the convergence of FL algorithms. By sampling more clients per round, we can observe a more representative sample of the underlying population—possibly reducing the number of communication rounds needed to achieve a given accuracy. This intuition is reflected in many convergence analyses (Khaled et al., 2019; 2020; Yang et al., 2021), which generally show that larger cohorts improve convergence.

Larger cohorts may also provide privacy benefits. Under the distributed differential privacy model (Shi et al., 2011; Bittau et al., 2017; Cheu et al., 2019; Erlingsson et al., 2020), noise is often added to the updates sent from the clients to the server (McMahan et al., 2018). By dividing the noise among more clients, larger cohorts may mitigate detrimental effects of noise. Since privacy tends to decrease as a function of the number of rounds (Abadi et al., 2016; Girgis et al., 2020), larger cohorts may also improve privacy by reducing the number of rounds needed for convergence.

Motivated by these potential benefits, we explore the impact of cohort size in realistic cross-device settings. We show that large-cohort training may not lead to significant convergence improvements in practice, as large-cohort training can introduce fundamental optimization issues. Our results are reminiscent of work on large-batch training in centralized settings, where larger batches can stagnate convergence improvements (Dean et al., 2012; You et al., 2017), and lead to generalization issues (Keskar et al., 2017; Hoffer et al., 2017). While some of the challenges we identify with are parallel to issues of large-batch training, others are unique to FL and have not been previously identified in the literature.

Contributions. In this work, we provide a novel examination of cohort sizes in federated learning. We give a wide ranging empirical analysis spanning many popular federated algorithms and datasets (Section 2). Despite the many possible benefits of large-cohort training, we find that challenges exist in realizing these benefits (Section 3). We show that these issues are caused in part by distinctive characteristics of federated training dynamics (Section 4). Using these insights, we provide partial solutions to the challenges we identify (Section 5), focusing on how to adapt techniques from large-batch training, and the limitations of such approaches. Our solutions are designed to serve as simple benchmarks for future work.

1.1. Related Work

Large-batch training. In centralized settings, mini-batch methods are common choices for training machine learning models. While larger mini-batch sizes ostensibly allow for improved convergence, in practice speedups may quickly saturate when increasing the mini-batch size. This property of diminishing returns has been explored both empirically (Dean et al., 2012; McCandlish et al., 2018; Golmant et al., 2018; Shallue et al., 2019) and theoretically (Ma et al., 2018; Yin et al., 2018). Beyond the issue of speedup saturation, numerous works have observed a *generalization gap* when training models with large batches (Keskar et al., 2017; Hoffer et al., 2017; You et al., 2017; Masters & Luschi, 2018; Lin et al., 2019; 2020). Our work differs from these areas by exploring how the cohort size (the number of selected clients) affects *federated* optimization methods.

Optimization for federated learning. There has been a large amount of work on developing federated optimization methods, often focusing on aspects such as communication-efficiency (Konečnỳ et al., 2016; McMahan et al., 2017), heterogeneity (Li et al., 2020a; Karimireddy et al., 2020b; Hsu et al., 2019), and fairness (Li et al., 2020c; Hu et al., 2020). We describe some relevant methods in Section 2, and defer to recent surveys for additional background (Kairouz et al., 2021; Li et al., 2020a). Our work is connected to variance reduction methods for FL, which can mitigate the effects of data heterogeneity (Karimireddy et al., 2020b;a; Zhang et al., 2020). Such methods may require clients to maintain state across rounds, or require high participation rates, both of which may be infeasible in cross-device settings (Kairouz et al., 2021). Convergence analyses of FL methods often show that larger cohorts improve convergence, even without explicit variance reduction (Khaled et al., 2019; 2020; Yang et al., 2021). These analyses typically focus on asymptotic convergence, and require assumptions that may not hold in practice (Kairouz et al., 2021). By contrast, we explore whether increased cohort sizes improve convergence in realistic, communication-limited settings.

Client sampling. A number of works have explored how to select cohorts of a fixed size in cross-device FL (Nishio & Yonetani, 2019; Goetz et al., 2019; Cho et al., 2020; Chen et al., 2020; Ribero & Vikalo, 2020). Such methods can yield faster convergence than random sampling by carefully selecting the clients that participate at each round, based on quantities such as the client loss. However, such approaches typically require the server to be able to choose which clients participate in a cohort. In practice, cohort selection in cross-device FL is often governed by client availability, and is not controlled by the server (Bonawitz et al., 2019; Paulik et al., 2021). In this work we instead focus on the impact of size of the cohort, assuming the cohort is sampled at random.

2. Preliminaries

Federated optimization methods often aim to minimize a weighted average of client loss functions:

$$\min_x f(x) := \sum_{k=1}^{K} p_k f_k(x), \tag{1}$$

where K is the total number of clients and f_k is the loss of client k. For practical reasons, p_k is often set to the number of examples in client k's local dataset (McMahan et al., 2017; Li et al., 2020b). To solve (1), each client in a cohort could send $\nabla f_k(x)$ to the server, and the server could perform mini-batch SGD. This approach, `FedSGD` (McMahan et al., 2017), requires communication for every model update, which may not be desirable. To address this, McMahan et al. (2017) propose `FedAvg`, in which clients perform multiple training steps, potentially reducing the number of communication rounds needed for convergence.

We focus on a generalized framework, `FedOpt`, introduced by Reddi et al. (2021) that uses client and server optimization. At each round, the server sends its model x to a cohort of clients C of size M. Each client $k \in C$ performs E epochs mini-batch SGD with client learning rate η_c, producing a local model x_k. The client then sends $\Delta_k := x_k - x$ to the server. The server computes a weighted average Δ of the client updates, and updates its own model via

$$x' = \textsc{ServerOpt}(x, \eta_s, \Delta)\,, \tag{2}$$

where $\textsc{ServerOpt}(x, \eta_s, g)$ is some first-order optimizer, η_s is the server learning rate, and g is a gradient estimate. The Δ in (2) is referred to as a **pseudo-gradient** (Reddi et al., 2021) since it is not an unbiased estimate of ∇f. Full pseudo-code of `FedOpt` is given in Algorithm 1.

Algorithm 1 `FedOpt` framework

Input: $M, T\ E, x^1, \eta_c, \eta_s, \textsc{ServerOpt}, \{p_k\}_{k=1}^K$
for $t = 1, \cdots, T$ **do**
  Server selects a cohort C_t of M clients uniformly at random, without replacement, and sends x^t to all clients in C_t.
  Each client $k \in C_t$ performs E epochs of mini-batch SGD on f_k with step-size η_c, obtaining a model x_k^t.
  Each client $k \in C_t$ sends $\Delta_k^t = x^t - x_k^t$ to the server.
  Server computes a pseudo-gradient Δ^t and updates its model:

$$\Delta^t = \frac{\sum_{k\in C_t} p_k \Delta_k^t}{\sum_{k\in C_t} p_k}, \quad x^{t+1} = \textsc{ServerOpt}(x_t, \eta_s, \Delta^t).$$

Algorithm 1 generalizes a number of FL algorithms, including `FedAvg` (McMahan et al., 2017), `FedAvgM` (Hsu et al., 2019), `FedAdagrad` (Reddi et al., 2021), and `FedAdam` (Reddi et al., 2021). These are the cases where SERVEROPT is SGD, SGD with momentum, Adagrad (McMahan & Streeter, 2010; Duchi et al., 2011), and

Table 1. Training dataset statistics.

DATASET	CLIENTS	EXAMPLES
CIFAR-100	500	50,000
EMNIST	3,400	671,585
SHAKESPEARE	715	16,068
STACK OVERFLOW	342,477	135,818,730

Adam (Kingma & Ba, 2015), respectively. `FedSGD` is realized when SERVEROPT is SGD, $\eta_c = 1$, $E = 1$, and each client performs full-batch gradient descent.

2.1. Experimental Setup

We explore the impact of the cohort size M on Algorithm 1 by performing a wide-ranging empirical evaluation across multiple datasets, models, and tasks. We discuss the key facets of our experiments below.

Datasets, models, and tasks. We use four datasets: CIFAR-100, EMNIST, Shakespeare, and Stack Overflow (see Appendix A.1 for details). For CIFAR-100, we use the client partitioning from (Reddi et al., 2021). The other three datasets have natural client partitions. The number of clients and examples in the training sets are given in Table 1.

For CIFAR-100, we train a ResNet-18, replacing batch normalization with group normalization (as proposed and validated by Hsieh et al. (2020)). For EMNIST, we train a convolutional network with two convolutional layers, max-pooling, dropout, and two dense layers. For Shakespeare, we train an RNN with two LSTM layers to perform next-character-prediction. For Stack Overflow, we perform next-word-prediction using an RNN with a single LSTM layer. For details on models and datasets, see Appendix A.1.

Algorithms. We implement special cases of Algorithm 1, including `FedSGD`, `FedAvg`, `FedAvgM`, `FedAdagrad`, and `FedAdam`. We also develop new methods, `FedLARS` and `FedLamb`, which are special cases of Algorithm 1 where SERVEROPT is LARS (You et al., 2017) and Lamb (You et al., 2020), respectively.

Implementation and tuning. Throughout, clients perform $E = 1$ epochs of training with mini-batch SGD. The batch size is fixed per-task, and p_k is the number of examples in client k's dataset. We tune learning rates for all algorithms using held-out validation data. We provide open-source implementations (link) of all simulations in TensorFlow Federated (Authors, 2019a) For more details, see Appendix A.

Presentation of results. For brevity, we present representative results to illustrate large-cohort training phenomena. See Appendix B for all experimental results. We run 5 random trials for each experiment, varying the model initialization and client sampling. In all figures, dark lines indicate the mean across 5 trials, and shaded regions indicate one standard deviation above and below the mean.

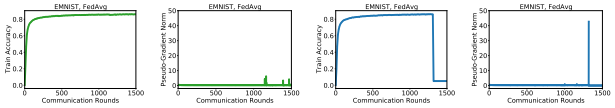

Figure 1. Applying `FedAvg` to EMNIST with cohort size 200. We plot the train accuracy and norm of the pseudo-gradient for a trial that ran successfully (**left**), and one that experienced a catastrophic training failure (**right**). The trials differed only in which clients were randomly sampled each round.

3. Large-Cohort Training Challenges

In this section we explore challenges that exist when using large cohorts in FL. While some of these challenges mirror issues in large-batch training, others are unique to federated settings.

3.1. Catastrophic Training Failures

Due to data heterogeneity, the server model x may perform poorly on a client's loss f_k, in which case $\nabla f_k(x)$ can blow up and lead to optimization problems. This issue is exacerbated by large cohorts, as we are more likely to sample misaligned clients. To demonstrate this, we apply `FedAvg` to EMNIST with varying cohort sizes M. For each M, we perform 5 trials and record whether a *catastrophic training failure* occurred, in which the training accuracy decreased by a factor of at least $1/2$ in a single round.

The failure rate increased from 0% for $M = 10$ to 80% for $M = 800$. When failures occurred, we saw a spike in the norm of the pseudo-gradient Δ (Figure 1). To prevent this, we use the *adaptive clipping* method of (Andrew et al., 2019). While this technique was designed for differential privacy, it greatly improved the stability of large-cohort training. Applying `FedAvg` to EMNIST with adaptive clipping, no catastrophic training failures occurred for any cohort size. We use adaptive clipping in all subsequent experiments. See Appendix A.3 for details.

3.2. Diminishing Returns

While increasing M in Algorithm 1 can improve convergence, these improvements diminish with M. To demonstrate this, we compute the test accuracy of `FedAvg` and `FedSGD` for varying cohort sizes M. Results for Stack Overflow are given in Figure 2.

The convergence benefits do not scale linearly with cohort size. While increasing M from 1 to 10 can significantly improve convergence, there is generally a threshold after which point increasing M incurs little to no change in convergence. We see comparable results for other tasks (despite

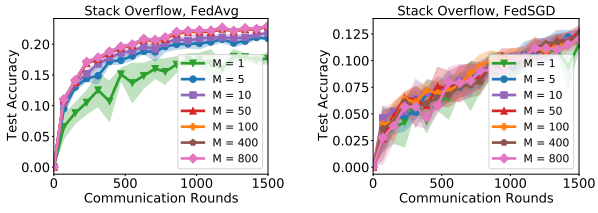

Figure 2. Test accuracy of `FedAvg` (left) and `FedSGD` (right) for various cohort sizes M on Stack Overflow.

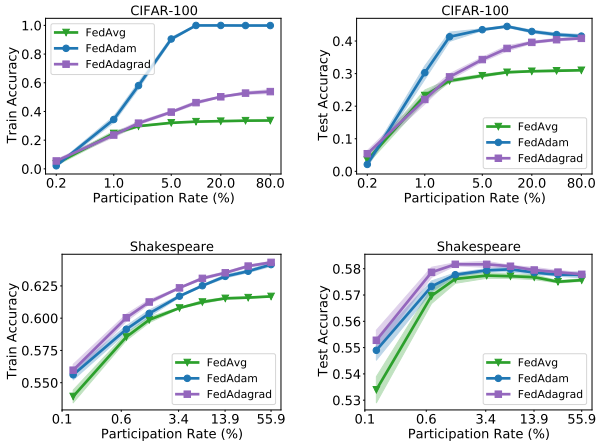

Figure 3. The train and test accuracy of `FedAvg`, `FedAdam`, and `FedAdagrad` on CIFAR-100 (left) and Shakespeare (right) after training for 1500 communication rounds, for varying cohort sizes. The x-axis denotes the percentage of training clients in each cohort.

having vastly different numbers of clients), as well as for other optimizers, including `FedAdam` and `FedAdagrad`. See Appendix B.1 for the full results. In short, increasing M alone can lead to *diminishing returns*, or even no returns in terms of convergence. This mirrors issues of diminishing returns in large-batch training (McCandlish et al., 2018).

3.3. Generalization Failures

Large-batch centralized optimization methods have repeatedly been shown to converge to models with worse generalization ability than models found by small-batch methods (Keskar et al., 2017; Hoffer et al., 2017; You et al., 2017; Masters & Luschi, 2018; Lin et al., 2019; 2020). Given the parallels between batch size in centralized learning and cohort size in FL, this raises obvious questions about whether similar issues occur in FL. In order to test this, we applied `FedAvg`, `FedAdam`, and `FedAdagrad` with different cohort sizes to various models. In Figure 3, we plot the train and test accuracy of each model after 1500 rounds.

Generalization issues do occur in FL. On Shakespeare, larger cohorts led to worse test accuracy for all three methods. For CIFAR-100, larger cohorts led to worse test accuracy for `FedAdam`, despite having similar training accuracy to modest cohort sizes. This resembles findings of Keskar et al. (2017), who show that large-batch training can reduce generalization. However, generalization issues do not occur uniformly. It is often optimizer-dependent (as in CIFAR-100) and does not occur on EMNIST and Stack Overflow (Appendix B.2). Notably, CIFAR-100 and Shakespeare have many fewer clients. Thus, large-cohort training may reduce generalization, especially when the cohort size is large compared to the total number of clients.

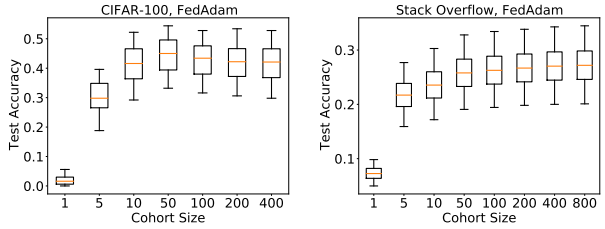

Figure 4. Accuracy of `FedAdam` after training for 1500 communication rounds on CIFAR-100 (left) and Stack Overflow (right). The box plots show the 5th, 25th, 50th, 75th, and 95th percentiles of accuracy across test clients.

3.4. Fairness Concerns

One critical issue in FL is fairness across clients, as minimizing (1) may disadvantage some clients (Mohri et al., 2019; Li et al., 2020c). Intuitively, large-cohort training methods may be better suited for ensuring fairness, since a greater fraction of the population is allowed to contribute to the model at each round. As a coarse measure of fairness, we compute percentiles of accuracy of our trained models across test clients. Fairer algorithms should lead to higher accuracy values for smaller percentiles. The percentiles for `FedAdam` on each task are given in Figure 4.

The cohort size seems to affect all percentiles in the same manner for a given task. On CIFAR-100, $M = 50$ performs the best for all percentiles. By contrast, for Stack Overflow (which has many more clients) $M = 800$ performed the best for all percentiles. This suggests a connection between fairness and the fraction of test clients participating at every round. See Appendix B.4 for more results.

3.5. Decreased Data Efficiency

Despite the challenges above, large-cohort training (especially with adaptive optimizers) often leads to faster convergence to given accuracy thresholds. In Figure 5, we see that the number of rounds `FedAdam` requires to reach certain accuracy thresholds generally decreases with the cohort size. While it is tempting to say that large-cohort training is therefore "faster", this ignores practical costs. Completing a single training round requires more resources with larger cohorts. To showcase this, we plot the accuracy of `FedAdam`

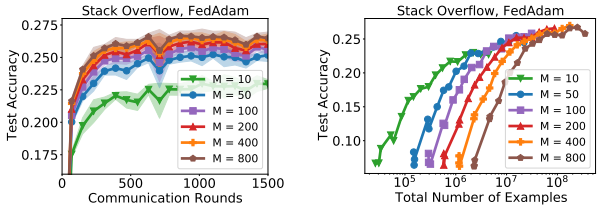

Figure 5. Test accuracy of `FedAdam` on Stack Overflow with various cohort sizes. We plot versus the number of communication rounds (left) and the number of examples processed (right).

with respect to the number of examples seen in Figure 5. This measures the data-efficiency of large-cohort training, and shows that large cohort-training requires significantly more examples per unit-accuracy.

While data-ineffiency also occurs in large-batch training (McCandlish et al., 2018), it is especially important in FL. In realistic cross-device settings client compute times can scale super-linearly with their amount of data, so clients with more data are more likely to become *stragglers* (Bonawitz et al., 2019). This straggler effect means that data-inefficient algorithms may require longer training times. We show in Appendix B.5 that under the straggler model from (Lee et al., 2017), large-cohort training can require significantly more compute time to converge.

4. Diagnosing Large-Cohort Challenges

A key difference between `FedAvg` and `FedSGD` is what the pseudo-gradient Δ in (1) represents. While Δ is an unbiased gradient estimate in `FedSGD`, this does not hold for `FedAvg` and related methods (Malinovskiy et al., 2020; Pathak & Wainwright, 2020; Charles & Konečný, 2021). While increasing the cohort size should reduce the variance of Δ, it is unclear what this quantity represents.

To better understand Δ, we plot its norm for `FedSGD` and `FedAvg` in Figures 6a and 6b. For `FedSGD`, $\|\Delta\|$ decreases slightly with M, but has high variance. For `FedAvg` larger cohorts lead to smaller norms. The decrease obeys an inverse square root rule: If Δ_1, Δ_2 are pseudo-gradients at some round for cohort sizes M_1, M_2, then $\|\Delta_1\|/\|\Delta_2\| \approx \sqrt{M_2/M_1}$. We use this rule to predict pseudo-gradient norms for `FedAvg` in Figure 6c. After a small number of rounds, we obtain a remarkably good approximation. To explain this, we plot the average cosine similarity between client updates Δ_k^t at each round in Figure 6d. For `FedAvg`, the client updates are almost orthogonal. This explains Figure 6b, as Δ is an average of nearly orthogonal vectors. Similar results hold for other tasks and optimizers (Appendix B.6).

Implications for large-cohort training. This near-orthogonality of client updates is key to understanding the

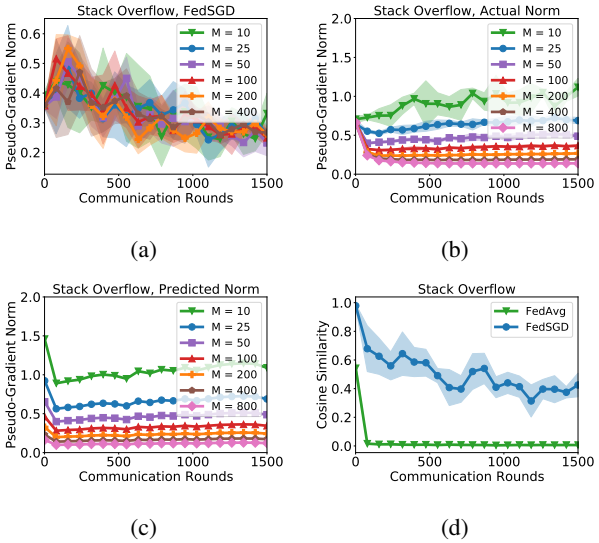

Figure 6. Pseudo-gradient norm of `FedSGD` (a) and `FedAvg` (b) on Stack Overflow. We plot the predicted norm for `FedAvg` using an inverse square root scaling rule relative to $M = 50$ (c) and the average cosine similarity of client updates for $M = 50$ (d).

challenges in Section 3. The diminishing returns in Section 3.2 occur in part because increasing M leads to smaller updates. This also sheds light on Section 3.5: In large-cohort training, we average of many nearly-orthogonal vectors, so each client's examples contribute little. Figure 6c also highlights an advantage of methods such as `FedAdam` and `FedAdagrad`: Adaptive server optimizers employ a form of normalization that makes them somewhat scale-invariant, compensating for the norm reduction.

5. Designing Better Methods

We now explore methods aimed at improving large-cohort training, drawing inspiration where possible from large-batch training.

Learning rate scaling. One common technique for large-batch training is to scale the learning rate according to the batch size. Two popular scaling methods are square root (Krizhevsky, 2014) and linear (Goyal et al., 2017) scaling. While such techniques have empirical benefits in centralized training, there are many different ways that they could be adapted to FL. We fix the client learning rate, and scale the server learning rate with the cohort size. We use square root and linear scaling rules: Given a learning rate η_s tuned for M, for $M' \geq M$ we use a learning rate η_s' where

$$\eta_s' = \eta_s \sqrt{M'/M} \quad \text{OR} \quad \eta_s' = \eta_s M'/M. \tag{3}$$

We also use a version of the warmup strategy from (Goyal et al., 2017), where we linearly increase the server learning rate from η_s to η_s' over the first 100 rounds. In our experiments, we use η_s tuned for $M = 50$. Our exper-

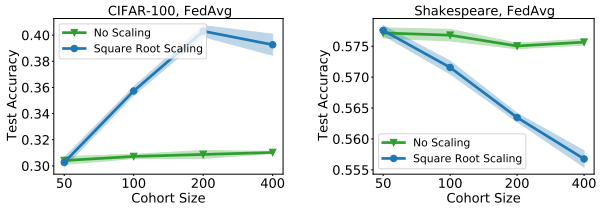

Figure 7. Test accuracy of `FedAvg` with and without square root scaling, on CIFAR-100 (left) and Shakespeare (right).

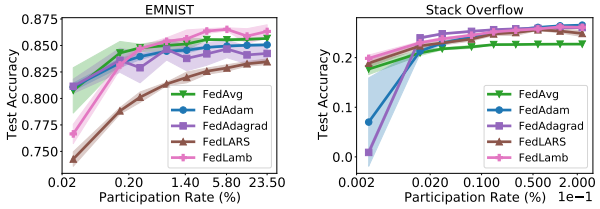

Figure 8. Test accuracy of various methods, including `FedLARS` and `FedLamb`, after 1500 rounds. The x-axis denotes percentage of training clients in each cohort.

iments show that server learning rate scaling has mixed efficacy. Linear scaling is often too aggressive for FL, and caused catastrophic training failures beyond $M = 100$ even with adaptive clipping. While square root scaling did not cause training failures, its performance (Figure 7) varied. It improved test accuracy for CIFAR-100, but decreased test accuracy for Shakespeare, despite improving the train accuracy for both. See Appendix B.7 for all results.

Layer-wise adaptivity. Another popular technique for large-batch training is *layer-wise adaptivity*. Methods such as LARS (You et al., 2017) and Lamb (You et al., 2020) use layer-wise adaptive learning rates, which may converge faster than SGD in large-batch settings (You et al., 2017; 2020). We propose two new federated versions of these optimizers, `FedLARS` and `FedLamb`, designed for large-cohort training. These are special cases of Algorithm 1, where the server uses LARS and Lamb, respectively.

In Figure 8, we present the accuracy of these methods. We see that `FedLamb` is generally comparable to `FedAdam` for large cohort sizes. One notable exception is Stack Overflow, in which `FedLamb` performs well even for $M = 1$. `FedLARS` has mixed performance, and does not do well on EMNIST or Shakespeare. For the full results, see Appendix B.1. While federated layer-wise adaptive algorithms can be better than coordinate-wise adaptive algorithms on certain datasets in some large-cohort settings, our results do not indicate that they are universally better.

Dynamic cohort sizes. In order to improve the data efficiency of large-cohort training, we may wish to use smaller cohorts in earlier optimization stages, and increase the cohort size over time. This technique is analogous to dynamic batch size techniques (Smith et al., 2018). We start with an initial cohort size of $M = 50$ and double the size every 300 rounds up to $M = 800$ (or the maximum population size if smaller). We plot the results for `FedAvg` and `FedAdam` on CIFAR-100 and Stack Overflow in Figure 9. See Appendix B.8 for results on all tasks.

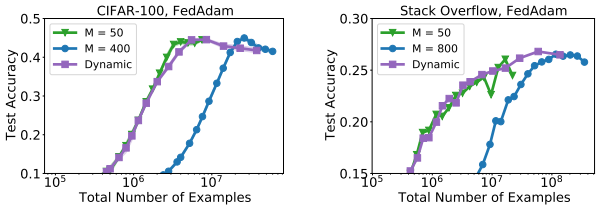

Figure 9. Test accuracy of `FedAdam` on CIFAR-100 (left) and Stack Overflow (right), with respect to the total number of examples processed, using fixed and dynamic cohort sizes.

This dynamic strategy attains data efficiency closer to a fixed cohort size of $M = 50$, while still obtaining a final accuracy closer to having used a large fixed cohort size. While our initial findings are promising, we note two important limitations. First, the accuracy of the dynamic strategy is bounded by the minimum and maximum cohort size used; It never attains a better accuracy than $M = 800$. Second, the doubling strategy still faces the generalization issues discussed in Section 3.3.

Other results. In Appendix B.9 we show that the number of local training steps is a key hyperparameter, and may need to be tuned in tandem with the cohort size. The number of local training steps in Algorithm 1 is a function of the number of training epochs and the client batch size, providing an interesting link between cohort sizes and batch sizes. We also propose a normalized version of `FedAvg`, in which we apply SGD to $\Delta/\|\Delta\|$. We show in Appendix B.10 that this can improve convergence in large-cohort training, obtaining similar performance to server learning rate scaling without introducing new hyperparameters.

6. Future Work

Future work involves connecting large-cohort training to other important aspects of FL, and continuing to explore connections with growing lines of work in large-batch training. In particular, we wish to see whether noising strategies, especially differential privacy mechanisms, can help overcome the generalization issues of large-cohort training. Personalization may also help mitigate issues of generalization and fairness. Finally, although not a focus of our work, we note that some of the findings above may extend to cross-silo settings, especially if communication restrictions require subsampling clients.

References

Abadi, M., Chu, A., Goodfellow, I., McMahan, H. B., Mironov, I., Talwar, K., and Zhang, L. Deep learning with differential privacy. In *Proceedings of the 2016 ACM SIGSAC Conference on Computer and Communications Security*, pp. 308–318, 2016.

Andrew, G., Thakkar, O., McMahan, H. B., and Ramaswamy, S. Differentially private learning with adaptive clipping. *arXiv preprint arXiv:1905.03871*, 2019.

Authors, T. T. TensorFlow Federated, 2019a. URL https://www.tensorflow.org/federated.

Authors, T. T. F. TensorFlow Federated Stack Overflow dataset, 2019b. URL https://www.tensorflow.org/federated/api_docs/python/tff/simulation/datasets/stackoverflow/load_data.

Bittau, A., Erlingsson, Ú., Maniatis, P., Mironov, I., Raghunathan, A., Lie, D., Rudominer, M., Kode, U., Tinnes, J., and Seefeld, B. PROCHLO: Strong privacy for analytics in the crowd. In *Proceedings of the 26th Symposium on Operating Systems Principles*, pp. 441–459, 2017.

Bonawitz, K., Eichner, H., Grieskamp, W., Huba, D., Ingerman, A., Ivanov, V., Kiddon, C., Konečný, J., Mazzocchi, S., McMahan, B., Van Overveldt, T., Petrou, D., Ramage, D., and Roselander, J. Towards federated learning at scale: System design. In *Proceedings of Machine Learning and Systems*. Proceedings of MLSys, 2019.

Caldas, S., Wu, P., Li, T., Konečný, J., McMahan, H. B., Smith, V., and Talwalkar, A. LEAF: A benchmark for federated settings. *arXiv preprint arXiv:1812.01097*, 2018.

Charles, Z. and Konečný, J. Convergence and accuracy trade-offs in federated learning and meta-learning. In *Proceedings of The 24th International Conference on Artificial Intelligence and Statistics*, 2021.

Chen, W., Horvath, S., and Richtarik, P. Optimal client sampling for federated learning. *arXiv preprint arXiv:2010.13723*, 2020.

Cheu, A., Smith, A., Ullman, J., Zeber, D., and Zhilyaev, M. Distributed differential privacy via shuffling. In *Annual International Conference on the Theory and Applications of Cryptographic Techniques*, pp. 375–403, 2019.

Cho, Y. J., Wang, J., and Joshi, G. Client selection in federated learning: Convergence analysis and power-of-choice selection strategies. *arXiv preprint arXiv:2010.01243*, 2020.

Cohen, G., Afshar, S., Tapson, J., and Van Schaik, A. EMNIST: Extending MNIST to handwritten letters. In *2017 International Joint Conference on Neural Networks (IJCNN)*, pp. 2921–2926. IEEE, 2017.

Dean, J., Corrado, G., Monga, R., Chen, K., Devin, M., Mao, M., Ranzato, M., Senior, A., Tucker, P., Yang, K., Le, Q., and Ng, A. Large scale distributed deep networks. In *Advances in Neural Information Processing Systems*, 2012.

Duchi, J., Hazan, E., and Singer, Y. Adaptive subgradient methods for online learning and stochastic optimization. *Journal of Machine Learning Research*, 12(Jul):2121–2159, 2011.

Erlingsson, Ú., Feldman, V., Mironov, I., Raghunathan, A., Song, S., Talwar, K., and Thakurta, A. Encode, shuffle, analyze privacy revisited: Formalizations and empirical evaluation. *arXiv preprint arXiv:2001.03618*, 2020.

Girgis, A. M., Data, D., Diggavi, S., Kairouz, P., and Suresh, A. T. Shuffled model of federated learning: Privacy, communication and accuracy trade-offs. *arXiv preprint arXiv:2008.07180*, 2020.

Goetz, J., Malik, K., Bui, D., Moon, S., Liu, H., and Kumar, A. Active federated learning. *arXiv preprint arXiv:1909.12641*, 2019.

Golmant, N., Vemuri, N., Yao, Z., Feinberg, V., Gholami, A., Rothauge, K., Mahoney, M. W., and Gonzalez, J. On the computational inefficiency of large batch sizes for stochastic gradient descent. *arXiv preprint arXiv:1811.12941*, 2018.

Goyal, P., Dollár, P., Girshick, R., Noordhuis, P., Wesolowski, L., Kyrola, A., Tulloch, A., Jia, Y., and He, K. Accurate, large minibatch SGD: Training ImageNet in 1 hour. *arXiv preprint arXiv:1706.02677*, 2017.

He, K., Zhang, X., Ren, S., and Sun, J. Deep residual learning for image recognition. In *Proceedings of the IEEE conference on computer vision and pattern recognition*, pp. 770–778, 2016.

Hochreiter, S. and Schmidhuber, J. Long short-term memory. *Neural Computation*, 9(8):1735–1780, 1997.

Hoffer, E., Hubara, I., and Soudry, D. Train longer, generalize better: closing the generalization gap in large batch training of neural networks. In *Advances in Neural Information Processing Systems*, 2017.

Hsieh, K., Phanishayee, A., Mutlu, O., and Gibbons, P. The non-IID data quagmire of decentralized machine learning. In *Proceedings of the 37th International Conference on Machine Learning*, 2020.

Hsu, T.-M. H., Qi, H., and Brown, M. Measuring the effects of non-identical data distribution for federated visual classification. *arXiv preprint arXiv:1909.06335*, 2019.

Hu, Z., Shaloudegi, K., Zhang, G., and Yu, Y. FedMGDA+: Federated learning meets multi-objective optimization. *arXiv preprint arXiv:2006.11489*, 2020.

Kairouz, P., McMahan, H. B., and contributors. Advances and open problems in federated learning. *Foundations and Trends® in Machine Learning*, 14(1), 2021. ISSN 1935-8237.

Karimireddy, S. P., Jaggi, M., Kale, S., Mohri, M., Reddi, S. J., Stich, S. U., and Suresh, A. T. Mime: Mimicking centralized stochastic algorithms in federated learning. *arXiv preprint arXiv:2008.03606*, 2020a.

Karimireddy, S. P., Kale, S., Mohri, M., Reddi, S., Stich, S., and Suresh, A. T. SCAFFOLD: Stochastic controlled averaging for federated learning. In *Proceedings of the 37th International Conference on Machine Learning*, 2020b.

Keskar, N. S., Mudigere, D., Nocedal, J., Smelyanskiy, M., and Tang, P. T. P. On large-batch training for deep learning: Generalization gap and sharp minima. In *International Conference on Learning Representations*, 2017.

Khaled, A., Mishchenko, K., and Richtárik, P. First analysis of local GD on heterogeneous data. *arXiv preprint arXiv:1909.04715*, 2019.

Khaled, A., Mishchenko, K., and Richtarik, P. Tighter theory for local SGD on identical and heterogeneous data. In *Proceedings of the Twenty Third International Conference on Artificial Intelligence and Statistics*, 2020.

Kingma, D. P. and Ba, J. Adam: A method for stochastic optimization. In *International Conference on Learning Representations*, 2015.

Konečnỳ, J., McMahan, H. B., Ramage, D., and Richtárik, P. Federated optimization: Distributed machine learning for on-device intelligence. *arXiv preprint arXiv:1610.02527*, 2016.

Krizhevsky, A. Learning multiple layers of features from tiny images. Technical report, 2009.

Krizhevsky, A. One weird trick for parallelizing convolutional neural networks. *arXiv preprint arXiv:1404.5997*, 2014.

Lee, K., Lam, M., Pedarsani, R., Papailiopoulos, D., and Ramchandran, K. Speeding up distributed machine learning using codes. *IEEE Transactions on Information Theory*, 64(3):1514–1529, 2017.

Li, T., Sahu, A. K., Talwalkar, A., and Smith, V. Federated learning: Challenges, methods, and future directions. *IEEE Signal Processing Magazine*, 37(3):50–60, 2020a.

Li, T., Sahu, A. K., Zaheer, M., Sanjabi, M., Talwalkar, A., and Smith, V. Federated optimization in heterogeneous networks. In *Proceedings of Machine Learning and Systems 2020*, pp. 429–450, 2020b.

Li, T., Sanjabi, M., Beirami, A., and Smith, V. Fair resource allocation in federated learning. In *International Conference on Learning Representations*, 2020c.

Li, W. and McCallum, A. Pachinko allocation: DAG-structured mixture models of topic correlations. In *Proceedings of the 23rd International Conference on Machine Learning*, 2006.

Liang, G. and Kozat, U. C. Tofec: Achieving optimal throughput-delay trade-off of cloud storage using erasure codes. In *IEEE INFOCOM 2014-IEEE Conference on Computer Communications*, 2014.

Lin, T., Stich, S. U., Patel, K. K., and Jaggi, M. Don't use large mini-batches, use local SGD. In *International Conference on Learning Representations*, 2019.

Lin, T., Kong, L., Stich, S., and Jaggi, M. Extrapolation for large-batch training in deep learning. In *Proceedings of the 37th International Conference on Machine Learning*, 2020.

Ma, S., Bassily, R., and Belkin, M. The power of interpolation: Understanding the effectiveness of SGD in modern over-parametrized learning. In *Proceedings of the 35th International Conference on Machine Learning*, 2018.

Malinovskiy, G., Kovalev, D., Gasanov, E., Condat, L., and Richtarik, P. From local SGD to local fixed-point methods for federated learning. In *Proceedings of the 37th International Conference on Machine Learning*, 2020.

Masters, D. and Luschi, C. Revisiting small batch training for deep neural networks. *arXiv preprint arXiv:1804.07612*, 2018.

McCandlish, S., Kaplan, J., Amodei, D., and Team, O. D. An empirical model of large-batch training. *arXiv preprint arXiv:1812.06162*, 2018.

McMahan, B., Moore, E., Ramage, D., Hampson, S., and Aguera y Arcas, B. Communication-efficient learning of deep networks from decentralized data. In *Proceedings of the 20th International Conference on Artificial Intelligence and Statistics*, volume 54, 2017.

McMahan, H. B. and Streeter, M. J. Adaptive bound optimization for online convex optimization. In *COLT The 23rd Conference on Learning Theory*, 2010.

McMahan, H. B., Ramage, D., Talwar, K., and Zhang, L. Learning differentially private recurrent language models. In *International Conference on Learning Representations*, 2018.

Mikolov, T., Karafiát, M., Burget, L., Černockỳ, J., and Khudanpur, S. Recurrent neural network based language model. In *Eleventh Annual Conference of the International Speech Communication Association*, 2010.

Mohri, M., Sivek, G., and Suresh, A. T. Agnostic federated learning. In *Proceedings of the 36th International Conference on Machine Learning*, 2019.

Nacson, M. S., Lee, J., Gunasekar, S., Savarese, P. H. P., Srebro, N., and Soudry, D. Convergence of gradient descent on separable data. In *The 22nd International Conference on Artificial Intelligence and Statistics*, 2019.

Nishio, T. and Yonetani, R. Client selection for federated learning with heterogeneous resources in mobile edge. In *IEEE International Conference on Communications (ICC)*, 2019.

Pathak, R. and Wainwright, M. J. FedSplit: An algorithmic framework for fast federated optimization. In *Advances in Neural Information Processing Systems*, pp. 7057–7066, 2020.

Paulik, M., Seigel, M., Mason, H., Telaar, D., Kluivers, J., van Dalen, R., Lau, C. W., Carlson, L., Granqvist, F., Vandevelde, C., et al. Federated evaluation and tuning for on-device personalization: System design & applications. *arXiv preprint arXiv:2102.08503*, 2021.

Reddi, S. J., Charles, Z., Zaheer, M., Garrett, Z., Rush, K., Konečný, J., Kumar, S., and McMahan, H. B. Adaptive federated optimization. In *International Conference on Learning Representations*, 2021.

Ribero, M. and Vikalo, H. Communication-efficient federated learning via optimal client sampling. *arXiv preprint arXiv:2007.15197*, 2020.

Shallue, C. J., Lee, J., Antognini, J., Sohl-Dickstein, J., Frostig, R., and Dahl, G. E. Measuring the effects of data parallelism on neural network training. *Journal of Machine Learning Research*, 20:1–49, 2019.

Shi, E., Chan, T. H., Rieffel, E., Chow, R., and Song, D. Privacy-preserving aggregation of time-series data. In *Proc. NDSS*, volume 2, pp. 1–17, 2011.

Smith, S. L., Kindermans, P.-J., and Le, Q. V. Don't decay the learning rate, increase the batch size. In *International Conference on Learning Representations*, 2018.

Wu, Y. and He, K. Group normalization. In *Proceedings of the European Conference on Computer Vision (ECCV)*, pp. 3–19, 2018.

Yang, H., Fang, M., and Liu, J. Achieving linear speedup with partial worker participation in non-IID federated learning. In *International Conference on Learning Representations*, 2021.

Yin, D., Pananjady, A., Lam, M., Papailiopoulos, D., Ramchandran, K., and Bartlett, P. Gradient diversity: a key ingredient for scalable distributed learning. In *Proceedings of the Twenty-First International Conference on Artificial Intelligence and Statistics*, 2018.

You, Y., Gitman, I., and Ginsburg, B. Large batch training of convolutional networks. *arXiv preprint arXiv:1708.03888*, 2017.

You, Y., Li, J., Reddi, S., Hseu, J., Kumar, S., Bhojanapalli, S., Song, X., Demmel, J., Keutzer, K., and Hsieh, C.-J. Large batch optimization for deep learning: Training bert in 76 minutes. In *International Conference on Learning Representations*, 2020.

Zhang, X., Hong, M., Dhople, S., Yin, W., and Liu, Y. FedPD: A federated learning framework with optimal rates and adaptivity to non-IID data. *arXiv preprint arXiv:2005.11418*, 2020.

A. Full Experimental Details

A.1. Datasets and Models

We use four datasets throughout our work: CIFAR-100 (Krizhevsky, 2009), the federated extended MNIST dataset (EMNIST) (Cohen et al., 2017), the Shakespeare dataset (Caldas et al., 2018), and the Stack Overflow dataset (Authors, 2019b). The first two datasets are image datasets, the second two are language datasets. All datasets are publicly available. We specifically use the versions available in TensorFlow Federated (Authors, 2019a), which gives a federated structure to all four datasets. Below we discuss the specifics of the dataset and classification task, as well as the model used to perform classification.

CIFAR-100 The CIFAR-100 dataset is a computer vision dataset consisting of $32 \times 32 \times 3$ images with 100 possible labels. While this dataset does not have a natural partition among clients, a federated version was created by Reddi et al. (2021) using hierarchical latent Dirichlet allocation to enforce moderate amounts of heterogeneity among clients. This partitioning among clients was based on Pachinko allocation (Li & McCallum, 2006). Note that under this partitioning, each client typically has only a subset of the 100 possible labels. The dataset has 500 training clients and 100 test clients, each with 100 examples in their local dataset.

We train a ResNet-18 (He et al., 2016) on this dataset, where we replace all batch normalization layers with group normalization layers (Wu & He, 2018). The use of group norm over batch norm in federated learning was first advocated by Hsieh et al. (2020), who showed that this helped improve classification accuracy in the presence of heterogeneous clients. We specifically use group normalization layers with two groups. We perform small amounts of data augmentation and preprocessing for each train and test sample. We first centrally crop each image $(24, 24, 3)$. We then normalize the pixel values according to their mean and standard deviation.

EMNIST The EMNIST dataset consists of images hand-written alphanumeric characters. Each image consists of 28×28 gray-scale pixel values. There are 62 total alphanumeric characters represented in the dataset. The images are partitioned among clients according to their author. The dataset has 3,400 clients, who have both train and test datasets. The dataset has natural heterogeneity stemming from the writing style of each person. We train a convolutional network on the dataset (the same one used by Reddi et al. (2021)). The network uses two convolutional layers (each with 3×3 kernels and strides of length 1), followed by a max pooling layer using dropout with $p = 0.25$, a dense layer with 128 units and dropout with $p = 0.5$, and a final dense output layer.

Shakespeare The Shakespeare dataset is derived from the benchmark designed by Caldas et al. (2018). The dataset corpus is the collected works of William Shakespeare, and the clients correspond to roles in Shakespeare's plays with at least two lines of dialogue. To eliminate confusion, *character* here will refer to alphanumeric characters (such as the letter *q*) and symbols such as punctuation, while we will use *client* to denote the various roles in plays (such as Macbeth). There are a total of 715 clients, whose lines are partitioned between train and test datasets.

We split each client's lines into sequences of 80 characters, padding if necessary. We use a vocabulary size of 90, where 86 characters are contained in Shakespeare's work, and the remaining 4 are beginning and end of line tokens, padding tokens, and out-of-vocabulary tokens. We perform next-character prediction on the clients' dialogue using a recurrent neural network (RNN) (Mikolov et al., 2010). We use the same model as Reddi et al. (2021). The RNN takes as input a sequence of 80 characters, embeds it into a learned 8-dimensional space, and passes the embedding through 2 LSTM layers (Hochreiter & Schmidhuber, 1997), each with 256 units. Finally, we use a softmax output layer with 80 units, where we try to predict a sequence of 80 characters formed by shifting the input sequence over by one. Therefore, our output dimension is 80×90. We compute loss using cross-entropy loss.

Stack Overflow Stack Overflow is a language dataset consisting of question and answers from the Stack Overflow site. The questions and answers also have associated metadata, including tags. Each client corresponds to a user. The specific train/validation/test split from (Authors, 2019b) has 342,477 train clients, 38,758 validation clients, and 204,088 test clients. Notably, the train clients only have examples from before 2018-01-01 UTC, while the test clients only have examples from after 2018-01-01 UTC. The validation clients have examples with no date restrictions, and all validation examples are held-out from both the test and train sets.

We perform next-word prediction on this dataset. We restrict each client to the first 1000 sentences in their dataset (if they

contain this many, otherwise we use the full dataset). We also perform padding and truncation to ensure that each sentence has 20 words. We then represent the sentence as a sequence of indices corresponding to the 10,000 most frequently used words, as well as indices representing padding, out-of-vocabulary words, the beginning of a sentence, and the end of a sentence. We perform next-word-prediction on these sequences using an a recurrent neural network (RNN) (Mikolov et al., 2010) that embeds each word in a sentence into a learned 96-dimensional space. It then feeds the embedded words into a single LSTM layer (Hochreiter & Schmidhuber, 1997) of hidden dimension 670, followed by a densely connected softmax output layer. Note that this is the same model used by Reddi et al. (2021). The metric used in the main body is the accuracy over the 10,000-word vocabulary; it does not include padding, out-of-vocab, or beginning or end of sentence tokens when computing the accuracy.

A.2. Implementation and Hyperparameters

We implement the previously proposed methods of `FedAvg`, `FedSGD`, `FedAvgM`, `FedAdam`, `FedAdagrad`, as well as two novel methods, `FedLARS` and `FedLamb`. All implementations are special cases of Algorithm 1. In all cases, clients use mini-batch SGD with batch size B. For `FedSGD`, the batch size B of a client is set to the size of its local dataset (so that the client only takes a single step). For all other optimizers, we fix B at a per-task level (see Table 2). Note that we use larger batch sizes for datasets where clients have more examples, like Stack Overflow. Except for the experiments in Appendix B.9, we set $E = 1$ throughout.

Table 2. Batch sizes used for each for all algorithms (except for `FedSGD`) on each dataset.

DATASET	BATCH SIZE
CIFAR-100	20
EMNIST	20
SHAKESPEARE	4
STACK OVERFLOW	32

For the actual implementation of the algorithms above, all methods (except for `FedSGD`) differ only in the choice of SERVEROPT in Algorithm 1. For `FedSGD`, in addition to having clients use full-batch SGD (as mentioned above), the client learning rate is set to be $\eta_c = 1$ in order to allow Algorithm 1 to recover the version of `FedSGD` proposed by McMahan et al. (2017). For all other algorithms, we present the choice of SERVEROPT and relevant hyperparameters (except for learning rates, see Section A.4) in Table 3. Note that here we use the notation from (Kingma & Ba, 2015), where β_1 refers to a first-moment momentum parameter, β_2 refers to a second-moment momentum parameter, and ϵ is a numerical stability constant used in adaptive methods. Note that for all adaptive methods, we set their initial accumulators to be 0.

Table 3. Hyperparameters and implementation details for all algorithms, relative to Algorithm 1. Here, β_1 denotes a first-moment momentum parameter, β_2 denotes a second-moment momentum parameter, and ϵ is a value used for numerical stability purposes in adaptive methods.

ALGORITHM	SERVEROPT	β_1	β_2	ϵ
`FedAvg` (McMahan et al., 2017)	SGD	0	N/A	N/A
`FedAvgM` (Hsieh et al., 2020)	SGD	0.9	N/A	N/A
`FedAdagrad` (Reddi et al., 2021)	Adagrad (Duchi et al., 2011)	N/A	N/A	0.001
`FedAdam` (Reddi et al., 2021)	Adam (Kingma & Ba, 2015)	0.9	0.99	0.001
`FedLARS`	LARS (You et al., 2017)	0.9	N/A	0.001
`FedLamb`	Lamb (You et al., 2020)	0.9	0.99	0.001

A.3. Adaptive Clipping

As exemplified in Figure 1, catastrophic training failures can occur when the server pseudo-gradient Δ^t is too large, which occurs more frequently for larger cohort sizes. To mitigate this issue, we use the adaptive clipping method proposed by

Andrew et al. (2019). While we encourage the reader to see this paper for full details and motivation, we give a brief overview of the method below.

Recall that in Algorithm 1, Δ^t is an average of client updates Δ_k^t. Thus, Δ^t can only be large if some client update is also large. In order to prevent this norm blow-up, we clip the client updates before averaging them. Rather than send Δ_k^t to the server, for a clipping level $\rho > 0$, the clients send $h(\Delta_k^t, \rho)$ where

$$h(v, \rho) = \begin{cases} v, & \text{if } \|v\| \leq \rho \\ \dfrac{\rho v}{\|v\|}, & \text{if } \|v\| > \rho. \end{cases}$$

Instead of fixing ρ a priori, we use the adaptive method proposed by Andrew et al. (2019). In this method, the clipping level varies across rounds, and is adaptively updated via a geometric update rule, where the goal is for ρ to estimate some norm percentile $q \in [0, 1]$. Notably, Andrew et al. (2019) show that the clipping level can be learned in a federated manner that is directly compatible with Algorithm 1. At each round t, let ρ^t be the clipping level (intended to estimate the qth percentile of norms across clients), and let C_t be the cohort of clients selected. Each client $k \in C_t$ computes their local model update Δ_k^t in the same manner as in Algorithm 1. Instead of sending Δ_k^t to the server, the client instead sends their clipped update $h(\Delta_k^t, \rho^t)$ to the server, along with $b_k^t := \mathbb{I}[\|\Delta_k^t\| \leq \rho^t]$, where $\mathbb{I}[A]$ denotes the indicator function of an event A. The server then computes:

$$\Delta^t = \frac{\sum_{k \in C_t} p_k h(\Delta_k^t)}{\sum_{k \in C_t} p_k}, \quad b^t = \frac{1}{|C_t|} \sum_{k \in C_t} b_k^t.$$

That is, Δ^t is a weighted average of the clipped client updates, and b^t is the fraction of unclipped client updates that did not exceed the clipping threshold. The server then updates its global model as in (2), but it also updates its estimate of the qth norm percentile using a learning rate $\eta_a > 0$ via

$$\rho^{t+1} = \rho^t \exp(-\eta_a (b^t - q)). \tag{4}$$

While Andrew et al. (2019) add noise in order to ensure that ρ is learned in a differentially private manner, we do not use such noise. Full pseudo-code combining Algorithm 1 and the adaptive clipping mechanisms discussed above is given in Algorithm 2.

Usage and hyperparameters. We use Algorithm 2 in all experiments (save for those in Figure 1, which illustrate the potential failures that can occur if clipping is not used). For hyperparameters, we use a target percentile of $q = 0.8$, with an initial clipping level of $\rho_1 = 1$. In our geometric update rule, we use a learning rate of $\eta_a = 0.2$.

A.4. Learning Rates and Tuning

For our experiments, we use client and server learning rates η_s, η_c that are tuned a priori on a held-out validation dataset. We tune both learning rates over $\{10^i \mid -3 \leq i \leq 1\}$ for each algorithm and dataset, therefore resulting in 25 possible configurations for each pair. This tuning, like the experiments following it, is based on the algorithm implementations discussed above. In particular, the tuning also uses the adaptive clipping framework discussed in Appendix A.3 and Algorithm 2.

While Stack Overflow has an explicit validation set distinct from the test and train datasets (Authors, 2019b), the other three datasets do not. In order to tune on these datasets, we randomly split the training clients (not the training examples!) into train and validation subsets according to an 80-20 split. We then use these federated datasets to perform held-out set tuning. We select the learning rates that have the best average validation performance after 1500 communication rounds with cohort size $M = 10$ over 5 random trials. A table of the resulting learning rates is given in Tables 4 and 5. Note that there is no client learning rate for `FedSGD`, as we must use $\eta_c = 1$ in Algorithm 1 in order to recover the version of `FedSGD` in (McMahan et al., 2017). Note that we use the same learning rates for all cohort sizes.

Algorithm 2 `FedOpt` framework with adaptive clipping

Input: M, T E, x^1, η_c, η_s, η_a, q, ρ^1, SERVEROPT, $\{p_k\}_{k=1}^K$
for $t = 1, \cdots, T$ **do**
The server selects a cohort C_t of M clients uniformly at random, without replacement.
The server sends x^t, ρ^t to all clients in C_t.
Each client $k \in C_t$ updates x^t for E epochs of mini-batch SGD with step-size η_c on f_k.
After training, each client has a local model x_k^t.
Each client $k \in C_t$ computes $\Delta_k^t = x^t - x_k^t$ and $b_k^t = \mathbb{I}[\|\Delta_k^t\| \leq \rho^t]$.
Each client $k \in C_t$ computes

$$h(\Delta_k^t) = \Delta_k^t \min\left\{1, \frac{\rho^t}{\|\Delta_k^t\|}\right\}.$$

Each client $k \in C_t$ sends $h(\Delta_k^t)$ and b_k^t to the server.
The server computes a pseudo-gradient Δ^t and updates its model via

$$\Delta^t = \frac{\sum_{k \in C_t} p_k h(\Delta_k^t)}{\sum_{k \in C_t} p_k}, \quad x^{t+1} = \text{SERVEROPT}(x_t, \eta_s, \Delta^t).$$

The server updates its clipping level via

$$b^t = \frac{1}{|C_t|} \sum_{k \in C_t} b_k^t, \quad \rho^{t+1} = \rho^t \exp(-\eta_a(b^t - q)).$$

Table 4. Server learning rate η_s used for each algorithm and dataset.

ALGORITHM	DATASET			
	CIFAR-100	EMNIST	Shakespeare	Stack Overflow
`FedAvg`	1	1	1	1
`FedAvgM`	1	1	0.1	1
`FedAdagrad`	0.01	0.1	0.1	10
`FedAdam`	0.01	0.001	0.01	1
`FedLARS`	0.01	0.001	0.01	0.01
`FedLamb`	0.001	0.01	0.01	0.01
`FedSGD`	0.1	0.1	1	10

B. Full Experiment Results

B.1. Test Accuracy Versus Communication Round

In this section, we present the test accuracy of various federated learning methods on various tasks, for various cohort sizes. The results are plotted in Figures 10, 11, 12, 13, 14, 15, and 16, which give the results for `FedSGD`, `FedAvg`, `FedAvgM`, `FedAdagrad`, `FedAdam`, `FedLARS`, and `FedLamb` (respectively).

Table 5. Client learning rate η_c used for each algorithm and dataset.

ALGORITHM	DATASET			
	CIFAR-100	EMNIST	Shakespeare	Stack Overflow
`FedAvg`	0.1	0.1	1	10
`FedAvgM`	0.1	0.1	1	10
`FedAdagrad`	0.1	0.001	10	10
`FedAdam`	0.1	0.1	10	10
`FedLARS`	0.1	0.1	10	1
`FedLamb`	0.01	0.1	10	10

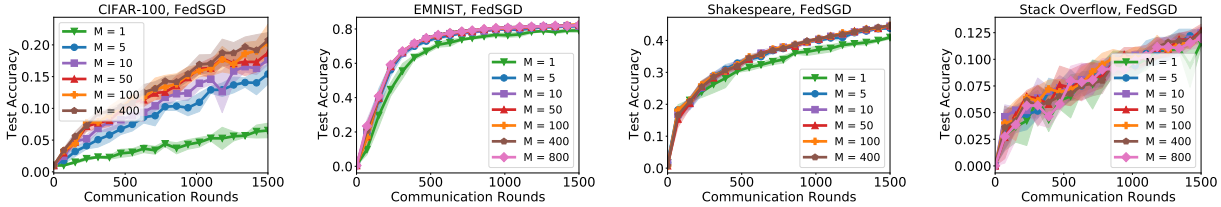

Figure 10. Average test accuracy of `FedSGD` versus the number of communication rounds, for various tasks and cohort sizes M.

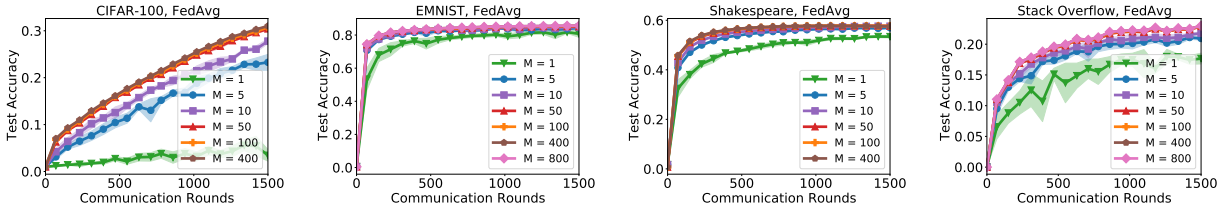

Figure 11. Average test accuracy of `FedAvg` versus the number of communication rounds, for various tasks and cohort sizes M.

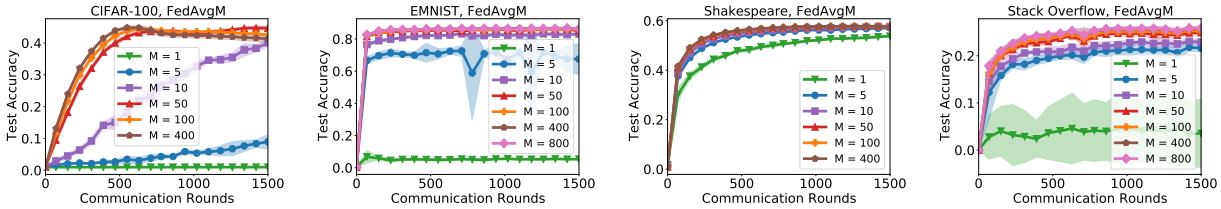

Figure 12. Average test accuracy of `FedAvgM` versus the number of communication rounds, for various tasks and cohort sizes M.

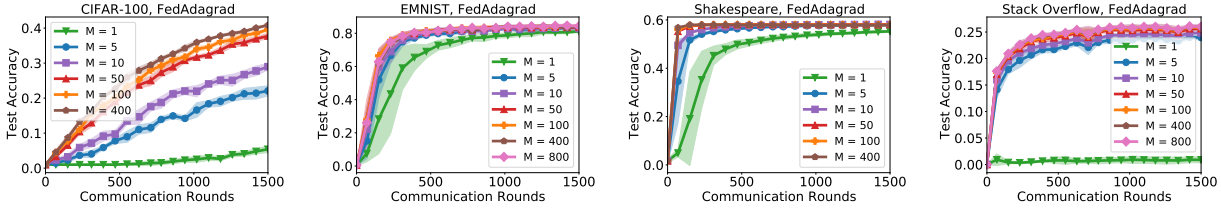

Figure 13. Average test accuracy of `FedAdagrad` versus the number of communication rounds, for various tasks and cohort sizes M.

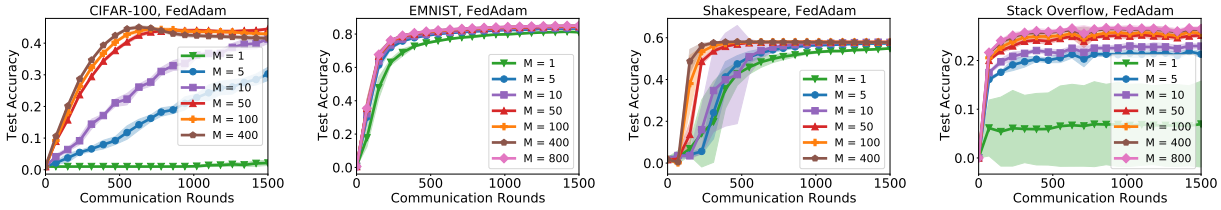

Figure 14. Average test accuracy of `FedAdam` versus the number of communication rounds, for various tasks and cohort sizes M.

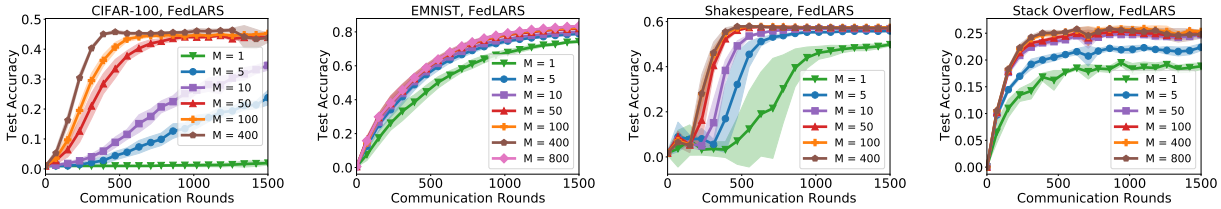

Figure 15. Average test accuracy of `FedLARS` versus the number of communication rounds, for various tasks and cohort sizes M.

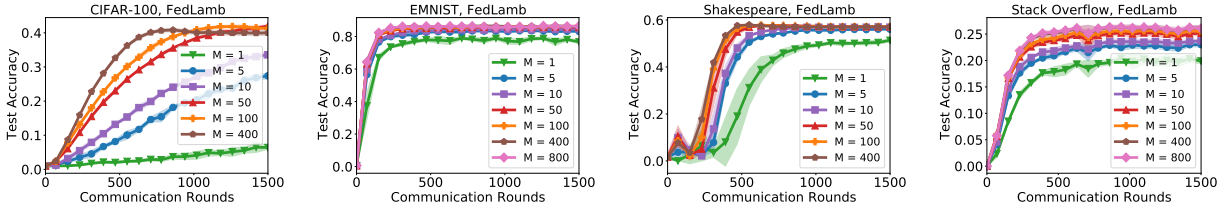

Figure 16. Average test accuracy of `FedLamb` versus the number of communication rounds, for various tasks and cohort sizes M.

B.2. Accuracy Versus Cohort Size

In this section, we showcase the train and test accuracy of various methods, as a function of the cohort size. The results are given in Figures 17 and 18, which correspond to the train and test accuracy, respectively. Both plots give the accuracy of `FedAvg`, `FedAdam`, `FedAdagrad`, `FedLARS`, and `FedLamb` as a function of the *participation rate*. That is, the percentage of training clients used in each cohort.

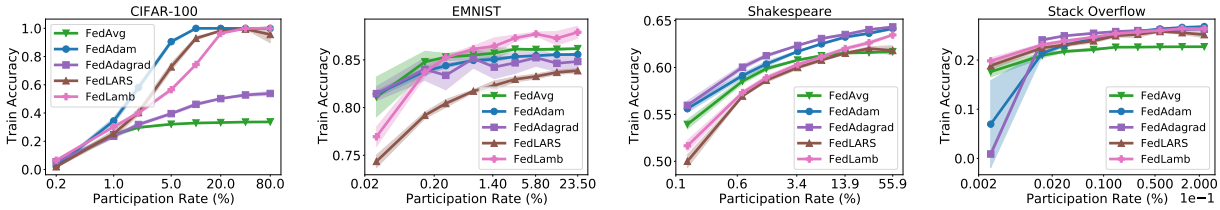

Figure 17. Train accuracy of `FedAvg`, `FedAdam`, `FedAdagrad`, `FedLARS`, and `FedLamb` after 1500 rounds, using varying cohort sizes and tasks. The x-axis denotes the percentage of training clients in each cohort.

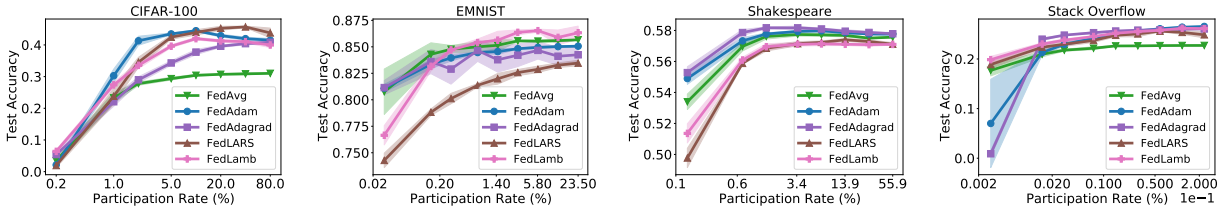

Figure 18. Test accuracy of `FedAvg`, `FedAdam`, `FedAdagrad`, `FedLARS`, and `FedLamb` after 1500 rounds, using varying cohort sizes and tasks. The x-axis denotes the percentage of training clients in each cohort.

B.3. Cohort Size Speedups

In this section, we attempt to see how much increasing the cohort size can speed up a federated algorithm. In particular, we plot the number of rounds needed to obtain a given accuracy threshold versus the cohort size. The results are given in Figures 19, 20, 21, 22, and 23. We see that in just about all cases, the speedups incurred by increasing the cohort size do not scale linearly. That being said, we still see that increasing the cohort size generally always leads to a reduction in the number of rounds needed to obtain a given test accuracy, and can lead to accuracy thresholds unobtainable by small-cohort training in communication-limited settings.

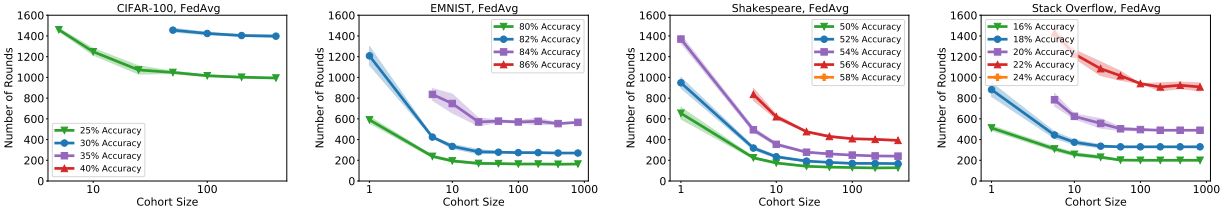

Figure 19. Number of communication rounds for `FedAvg` to obtain certain test accuracy thresholds. The x-axis denotes the cohort size.

While theory shows that in the worst-case, the cohort size leads to linear speedups, we find that this is generally not the case in practice.

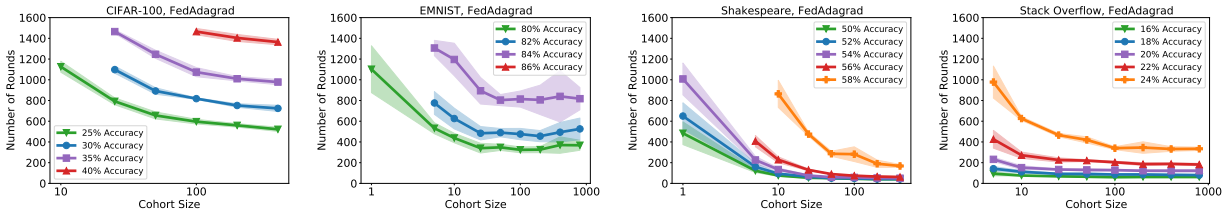

Figure 20. Number of communication rounds for `FedAdagrad` to obtain certain test accuracy thresholds. The x-axis denotes the cohort size.

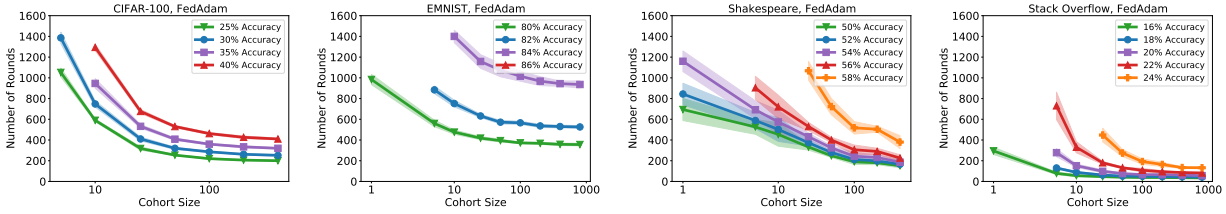

Figure 21. Number of communication rounds for `FedAdam` to obtain certain test accuracy thresholds. The x-axis denotes the cohort size.

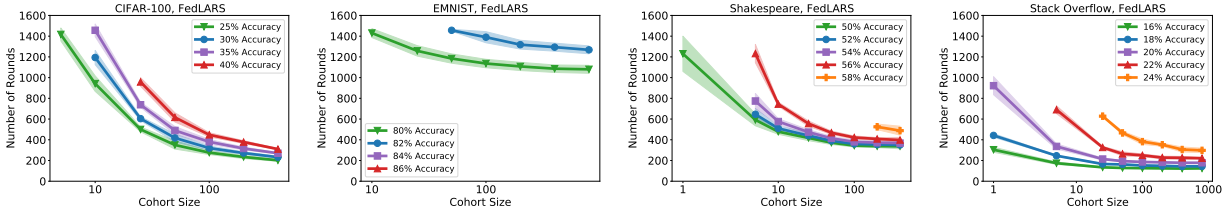

Figure 22. Number of communication rounds for `FedLARS` to obtain certain test accuracy thresholds. The x-axis denotes the cohort size.

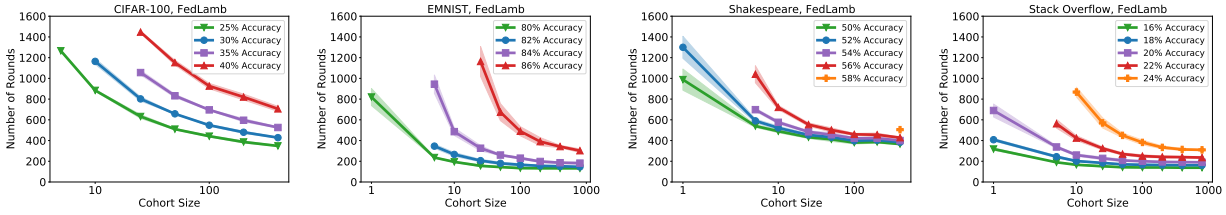

Figure 23. Number of communication rounds for `FedLamb` to obtain certain test accuracy thresholds. The x-axis denotes the cohort size.

B.4. Measures of Accuracy Across Clients

In this section, we expand on the fairness results in Section 3. In Tables 6, 7, 8, and 9, we present percentiles of accuracy of `FedAdam` across all test clients (after training for 1500 rounds, with varying cohort sizes and on varying tasks). For example, the 50th percentile of accuracy is the median accuracy of the learned model across all test clients.

The results show that in nearly all cases, the cohort size impacts all percentiles of accuracy in the same manner. For example, in Table 6, we see that a cohort size of $M = 50$ is better than other cohort sizes, for all percentiles of test accuracy. Notably, this does not support the notion that larger cohorts learn more fair models. Instead, it seems that large cohorts can lead to generalization failures across all percentiles, as it does on CIFAR-100 and Shakespeare (Tables 6 and 8). However, this does not occur on EMNIST and Stack Overflow (Tables 7 and 9), which have many more train and test clients.

Table 6. Percentiles of accuracy across test clients for `FedAdam` on CIFAR-100 after 1500 communication rounds. We present the mean and standard deviation across 5 random trials, with the largest accuracy values for each percentile in bold.

Percentile	Cohort Size				
	10	50	100	200	400
5	27.0 ± 3.3	$\mathbf{32.2 \pm 1.1}$	30.6 ± 0.9	29.6 ± 1.1	29.0 ± 1.2
25	35.3 ± 1.5	$\mathbf{39.0 \pm 0.7}$	37.5 ± 0.9	37.2 ± 1.1	36.4 ± 1.1
50	41.1 ± 1.3	$\mathbf{44.5 \pm 0.5}$	43.1 ± 0.7	42.4 ± 0.5	41.6 ± 0.7
75	47.5 ± 1.1	$\mathbf{50.1 \pm 0.7}$	48.4 ± 0.5	47.2 ± 0.4	47.0 ± 1.0
95	54.2 ± 1.5	$\mathbf{55.6 \pm 1.5}$	54.6 ± 1.5	53.8 ± 1.3	53.6 ± 1.5

Table 7. Percentiles of accuracy across test clients for `FedAdam` on EMNIST after 1500 communication rounds. We present the mean and standard deviation across 5 random trials, with the largest accuracy values for each percentile in bold.

Percentile	Cohort Size					
	10	50	100	200	400	800
5	61.9 ± 2.1	62.5 ± 2.4	64.3 ± 1.2	63.8 ± 1.4	64.3 ± 1.0	$\mathbf{65.0 \pm 0.9}$
25	77.3 ± 0.7	77.4 ± 1.4	77.9 ± 0.4	78.2 ± 0.4	78.6 ± 0.5	$\mathbf{78.7 \pm 0.3}$
50	84.5 ± 0.5	85.4 ± 0.5	85.9 ± 0.2	85.9 ± 0.2	86.1 ± 0.2	$\mathbf{86.2 \pm 0.1}$
75	91.2 ± 0.2	92.0 ± 0.1	92.0 ± 0.2	92.3 ± 0.1	92.3 ± 0.1	$\mathbf{92.3 \pm 0.0}$
95	100.0 ± 0.0	100.0 ± 0.0	100.0 ± 0.0	100.0 ± 0.0	100.0 ± 0.0	$\mathbf{100.0 \pm 0.0}$

Table 8. Percentiles of accuracy across test clients for `FedAdam` on Shakespeare after 1500 communication rounds. We present the mean and standard deviation across 5 random trials, with the largest accuracy values for each percentile in bold.

Percentile	Cohort Size				
	10	50	100	200	400
5	$\mathbf{39.9 \pm 0.8}$	39.2 ± 1.8	39.4 ± 1.6	37.8 ± 0.7	38.6 ± 1.2
25	54.9 ± 0.1	$\mathbf{55.0 \pm 0.2}$	54.9 ± 0.2	54.9 ± 0.1	54.9 ± 0.2
50	58.3 ± 0.2	58.5 ± 0.2	$\mathbf{58.5 \pm 0.2}$	58.3 ± 0.1	58.4 ± 0.1
75	61.8 ± 0.2	$\mathbf{62.4 \pm 0.2}$	62.2 ± 0.2	62.1 ± 0.2	62.1 ± 0.3
95	70.9 ± 0.6	$\mathbf{71.2 \pm 0.6}$	71.2 ± 0.4	71.1 ± 0.2	71.1 ± 0.2

Table 9. Percentiles of accuracy across test clients for `FedAdam` on Stack Overflow after 1500 communication rounds. We present the mean and standard deviation across 5 random trials, with the largest accuracy values for each percentile in bold.

Percentile	Cohort Size					
	10	50	100	200	400	800
5	16.7 ± 0.2	18.7 ± 0.2	19.1 ± 0.2	19.5 ± 0.1	19.8 ± 0.1	$\mathbf{19.9 \pm 0.1}$
25	21.0 ± 0.3	23.2 ± 0.2	23.6 ± 0.2	24.1 ± 0.1	24.4 ± 0.1	$\mathbf{24.5 \pm 0.1}$
50	23.5 ± 0.3	25.8 ± 0.2	26.3 ± 0.3	26.7 ± 0.1	27.0 ± 0.1	$\mathbf{27.2 \pm 0.1}$
75	26.1 ± 0.3	28.4 ± 0.2	29.0 ± 0.3	29.4 ± 0.1	29.7 ± 0.1	$\mathbf{29.9 \pm 0.1}$
95	30.8 ± 0.3	33.2 ± 0.2	33.7 ± 0.4	34.2 ± 0.1	34.6 ± 0.1	$\mathbf{34.8 \pm 0.1}$

B.5. Simulating Straggler Effects

As shown in Section 3.5, large-cohort training methods seem to face data-efficiency issues, where training with large cohorts requires processing many more examples to reach accuracy thresholds than small-cohort training. While this is related to diminishing returns (Section 3.2) and occurs in large-batch training as well (Golmant et al., 2018), we highlight this issue due to its consequences in federated learning.

Unlike centralized learning, federated learning faces fundamental limits on parallelization. Since data cannot be shared, we typically cannot scale up to arbitrarily large cohort sizes. Instead, the parallelization is limited by the available training clients. In order to learn on a client's local dataset, that client must actually perform the training on its examples. Unfortunately,

since clients are often lightweight in cross-device settings (Kairouz et al., 2021), clients with many examples may require longer compute times, becoming stragglers in a given communication round. If an algorithm is data-inefficient, these straggler clients may have to participate many times throughout training, causing the overall runtime to be greater. In short, data inefficiency can dramatically slow down large-cohort training algorithms.

To exemplify this, we compute simulated runtimes of federated algorithms under a version of the probabilistic straggler model from (Lee et al., 2017). We model each client's runtime as a random variable drawn from a shifted exponential distribution. Such models were found to be good models of runtimes for file queries in cloud storage systems (Liang & Kozat, 2014) and mini-batch SGD on distributed compute systems (Lee et al., 2017).

In our model, we assume that the time a client requires to perform local training is some constant proportional to the number of examples the client has, plus an exponential random variable. More formally, let N_k denote the number of examples held by some client k, and let X_k denote the amount of time required by client k to perform their local training in Algorithm 1. Then we assume that there are constants $\alpha, \lambda > 0$ such that

$$X_k - \alpha N_k \sim \text{Exp}\left(\frac{1}{\lambda N_k}\right).$$

Here λ is the *straggler parameter*. Recall that if $X \sim \text{Exp}(1/\lambda)$, then $\mathbb{E}[X] = \lambda$. Therefore, we assume that the expected runtime of client k equal αN plus some random variable whose expected value is λN. Thus, larger λ means larger expected client runtimes. By convention, we can also use $\lambda = 0$ in which case $X_k = \alpha N_k$. For a given round t of Algorithm 1, let C_t denote the cohort sampled. Since Algorithm 1 requires all clients to finish before updating its global model, we model the runtime Y_t of round t as

$$Y_t = \max_{k \in C_t} \{X_k\}.$$

Thus, the round runtime is the maximum of M shifted exponential random variables, where M is the cohort size. Note that this only models the client computation time, not the server computation time or communication time. Using this model, we plot the simulated runtime of `FedAvg` on various tasks, for varying cohort sizes. For simplicity, we assume $\alpha = 1$ in all experiments, and vary λ over $\{0.1, 1, 10, 100\}$. To showcase how much longer the runtime of large-cohort training may be, we present the simulated runtime, *relative* to $M = 10$. For $a \in [0, 1]$, we plot the ratio of how long it takes to reach a test accuracy of a with a cohort size of M, versus how long it takes to reach a with $M = 10$. We give the results for CIFAR-100, EMNIST, Shakespeare, and Stack Overflow in Figures 24, 25, 26, 27, respectively.

When λ is small, we see that larger cohorts can obtain higher test accuracy in a comparable amount of time to $M = 10$. However, when λ is large, large-cohort training may require anywhere from 5-10 times more client compute time. This is particularly important in cross-device settings with lightweight edge devices, as the straggler effect (which essentially increases with λ) may be larger. Note that we see particularly large increases in relative runtimes for smaller accuracy thresholds, which suggests that the dynamic cohort strategy from Section 5 may be useful in helping mitigate such issues.

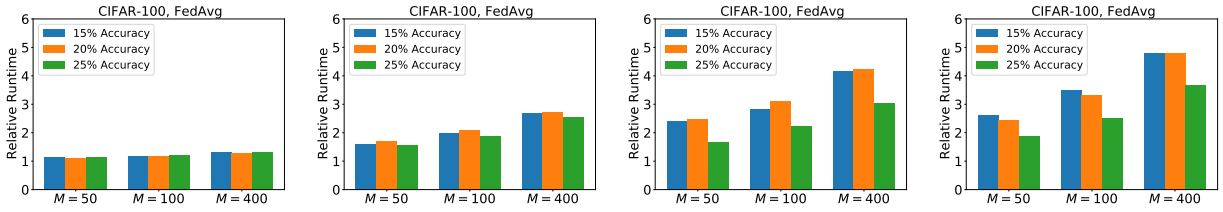

(a) $\lambda = 0.1$ (b) $\lambda = 1$ (c) $\lambda = 10$ (d) $\lambda = 100$

Figure 24. The relative amount of time required to reach given test accuracies on CIFAR-100 with varying cohort sizes. We present the ratio of the runtime needed for $M > 10$ with respect to the time needed for $M = 10$. Runtimes are simulated under a shifted exponential model with $\alpha = 1$ and varying λ.

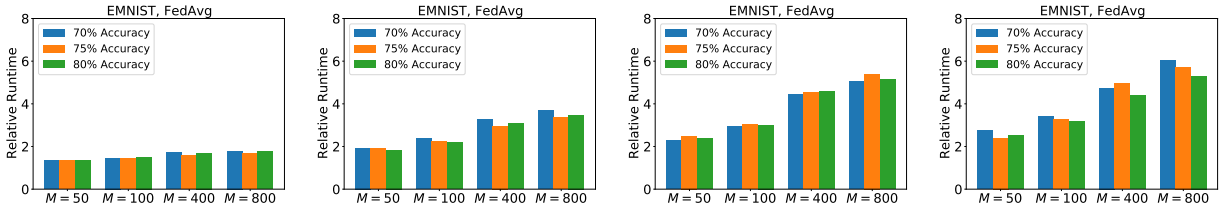

(a) $\lambda = 0.1$ (b) $\lambda = 1$ (c) $\lambda = 10$ (d) $\lambda = 100$

Figure 25. The relative amount of time required to reach given test accuracies on EMNIST with varying cohort sizes. We present the ratio of the runtime needed for $M > 10$ with respect to the time needed for $M = 10$. Runtimes are simulated under a shifted exponential model with $\alpha = 1$ and varying λ.

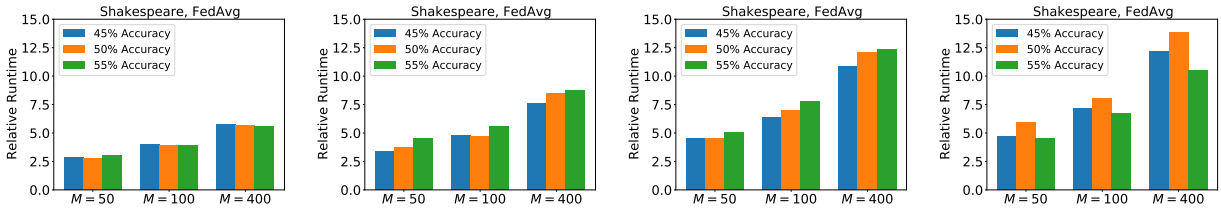

(a) $\lambda = 0.1$ (b) $\lambda = 1$ (c) $\lambda = 10$ (d) $\lambda = 100$

Figure 26. The relative amount of time required to reach given test accuracies on Shakespeare with varying cohort sizes. We present the ratio of the runtime needed for $M > 10$ with respect to the time needed for $M = 10$. Runtimes are simulated under a shifted exponential model with $\alpha = 1$ and varying λ.

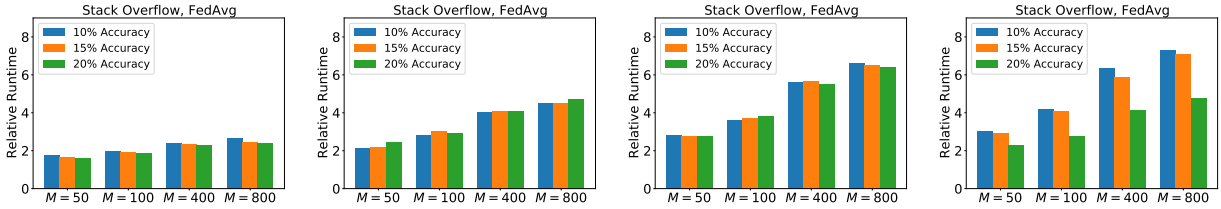

(a) $\lambda = 0.1$ (b) $\lambda = 1$ (c) $\lambda = 10$ (d) $\lambda = 100$

Figure 27. The relative amount of time required to reach given test accuracies on Stack Overflow with varying cohort sizes. We present the ratio of the runtime needed for $M > 10$ with respect to the time needed for $M = 10$. Runtimes are simulated under a shifted exponential model with $\alpha = 1$ and varying λ.

B.6. Pseudo-Gradient Norms

In this section, we present the norm of the server pseudo-gradient Δ in Algorithm 1 with respect to the number of communication rounds. We do this for varying cohort sizes and tasks across 1500 communication rounds. All plots give the ℓ_2 norm of Δ. The results are given in Figures 28, 29, 30, 31, 32, 33, and 34. These gives the results for `FedSGD`, `FedAvg`, `FedAvgM`, `FedAdagrad`, `FedAdam`, `FedLARS`, and `FedLamb` (respectively).

We find that in nearly all cases, the results for `FedSGD` differ from all other algorithms. While there is significant overlap in the pseudo-gradient norm for `FedSGD` across all cohort sizes (Figure 28), any method that uses multiple local training steps generally does not see such behavior. The only notable counter-example is `FedAdagrad` on EMNIST (Figure 31). Otherwise, both non-adaptive and adaptive federated methods that use local training (such as `FedAvg`, `FedAdam`, and `FedLamb`) see similar behavior: The pseudo-gradient norm is effectively stratified by the cohort size. Larger cohort sizes lead to smaller pseudo-gradient norms, with little overlap. Moreover, as discussed in Section 4, we see that after enough communication rounds occur, the pseudo-gradient norm obeys an inverse square root scaling rule.

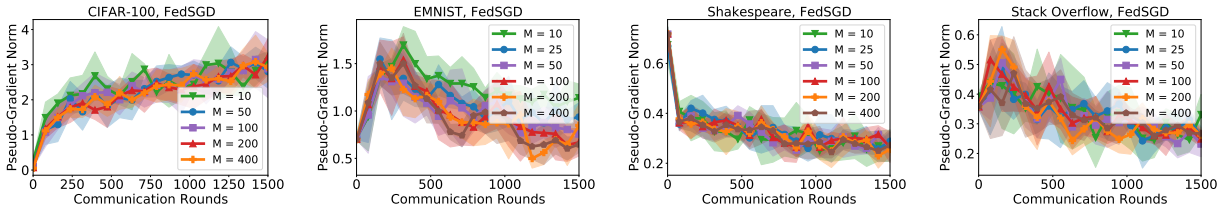

Figure 28. Average pseudo-gradient norm of `FedSGD` versus the number of communication rounds, for various tasks and cohort sizes M.

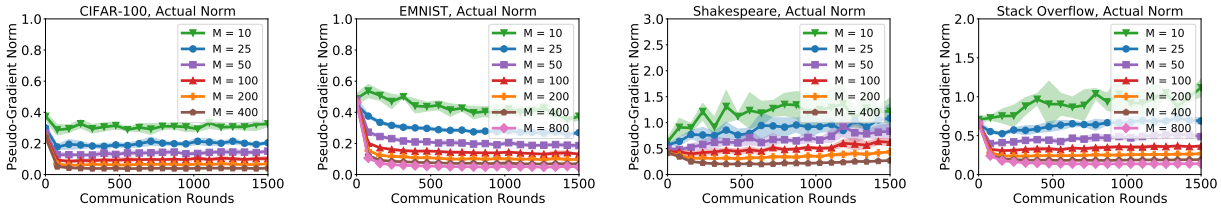

Figure 29. Average pseudo-gradient norm of `FedAvg` versus the number of communication rounds, for various tasks and cohort sizes M.

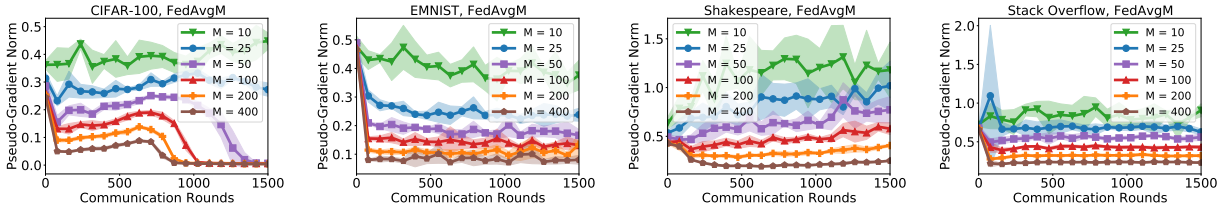

Figure 30. Average pseudo-gradient norm of `FedAvgM` versus the number of communication rounds, for various tasks and cohort sizes M.

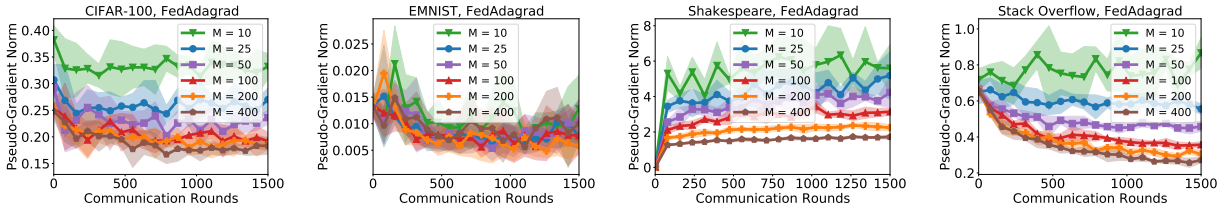

Figure 31. Average pseudo-gradient norm of `FedAdagrad` versus the number of communication rounds, for various tasks and cohort sizes M.

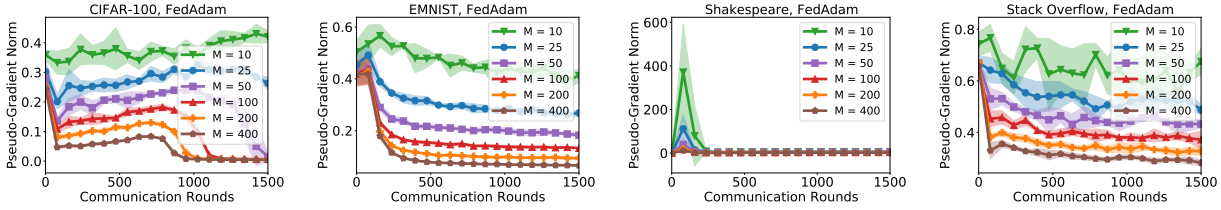

Figure 32. Average pseudo-gradient norm of `FedAdam` versus the number of communication rounds, for various tasks and cohort sizes M.

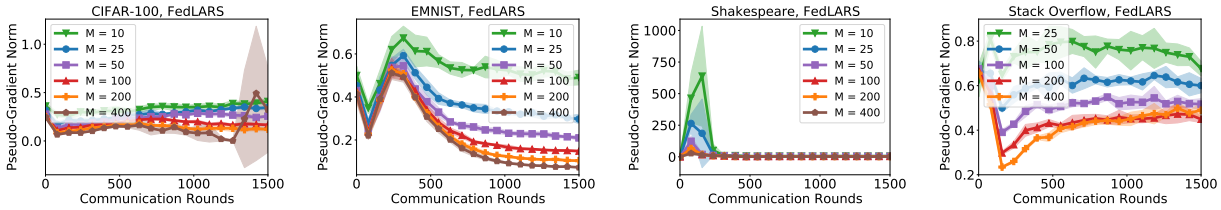

Figure 33. Average pseudo-gradient norm of `FedLARS` versus the number of communication rounds, for various tasks and cohort sizes M.

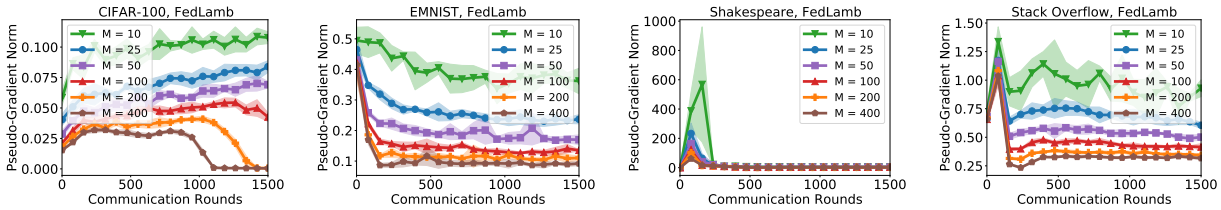

Figure 34. Average pseudo-gradient norm of `FedLamb` versus the number of communication rounds, for various tasks and cohort sizes M.

B.6.1. Cosine Similarity of Client Updates

Recall that in Section 4, we showed that for `FedAvg`, client updates are nearly orthogonal on the Stack Overflow task. In this section, we show that this holds across tasks. In Figure 35, we present the average cosine similarity between distinct clients in each training round, for `FedAvg` and `FedSGD`. Thus, given a cohort size M, at each round t we compute $\binom{|M|}{2}$ cosine similarities between client updates, and take the average over all pairs. Formally, we compute, for each round t,

$$\theta_t := \binom{|C_t|}{2}^{-1} \sum_{\substack{i,j \in C_t \\ i \neq j}} \frac{\left\langle \Delta_i^t, \Delta_j^t \right\rangle}{\|\Delta_i^t\|_2 \|\Delta_j^t\|_2} \tag{5}$$

where C_t is the cohort of sampled clients in round t, and Δ_k^t denotes the client update of client $k \in C_t$ (see Algorithm 1). Note that because we normalize, it does not matter whether we use clipping or not (Algorithm 2). The results for θ_t with cohort size $M = 50$ are given in Figure 35.

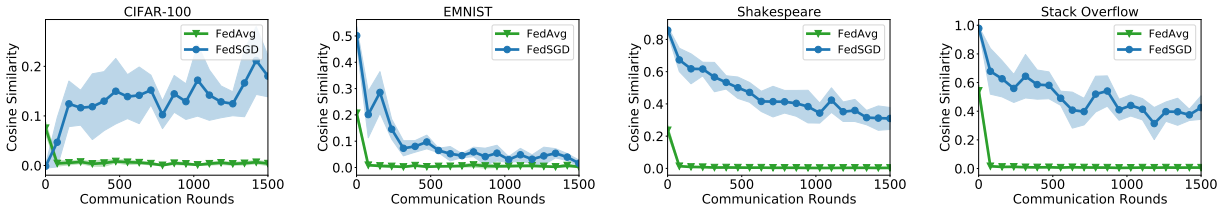

Figure 35. Average cosine similarity θ_t (as in (5)) between client updates Δ_k^t with respect to the number of communication rounds, for `FedAvg` on EMNIST with a cohort size of $M = 50$.

We see that in all cases, after a small number of communication rounds, θ_t becomes close to zero for `FedAvg`. By contrast, θ_t is not nearly as small for `FedSGD`, especially in intermediate rounds. We note that for EMNIST, the cosine similarity for `FedSGD` approaches that of `FedAvg` as $T \to 1500$.

B.7. Server Learning Rate Scaling

In this section, we present our full results using the learning rate scaling methods proposed in Section 5. Recall that our methods increase the server learning rate η_s in accordance with the cohort size. To do so, we fix a learning rate η_s for some cohort size M. As in (3), for $M' \geq M$, we use a server learning rate η_s'

$$\eta_s' = r\left(\frac{M'}{M}\right)\eta_s$$

where $r : \mathbb{R}_{\geq 0} \to \mathbb{R}_{\geq 0}$ determines the scaling rate. In particular, we focus on $r(a) = \sqrt{a}$ (square root scaling) and $r(a) = a$ (linear scaling). These rules both can be viewed as federated analogs of learning rate scaling techniques used for large-batch training (Krizhevsky, 2014; Goyal et al., 2017). We use them with a federated version of the warmup technique proposed by Goyal et al. (2017), where we linearly increase the server learning rate from 0 to η_s' over the first $W = 100$ communication rounds.

Despite the historical precedent for the linear scaling rule (Goyal et al., 2017), we find that it leads to catastrophic training failures in the federated regime, even with adaptive clipping. To showcase this, we plot the accuracy of `FedAvg` on EMNIST with the linear scaling rule in Figure 36. We plot the test accuracy over time, averaged across 5 random trials, for various cohort sizes M. While $M = 50, 100$ see similar convergence as in Figure 11, for $M = 200$, we saw one catastrophic training failure across all 5 trials. Using $M \geq 400$, we found that all trials resulted in catastrophic training failures. In short, linear scaling can be too aggressive in federated settings, potentially due to heterogeneity among clients (which intuitively requires some amount of conservatism in server model updates).

By contrast, the square root scaling rule did not lead to such training failures. We plot the training accuracy and test accuracy of `FedAvg` using the square root scaling rule in Figure 37. We plot this with respect to the cohort size, with and without the scaling rule. We see that the performance of the scaling rule is decidedly mixed. While it leads to significant improvements in training accuracy for CIFAR-100 and Shakespeare, it leads to only minor improvements (or a degradation in training

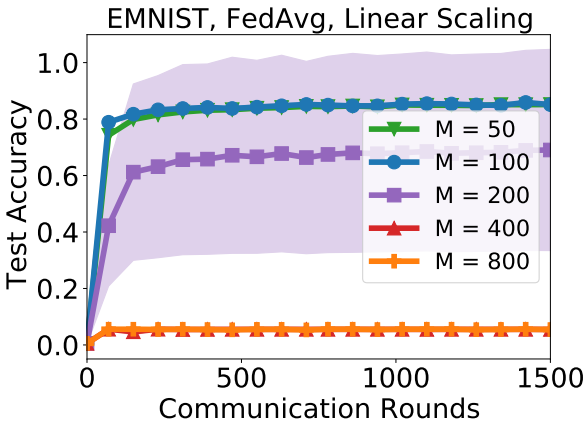

Figure 36. The test accuracy of `FedAvg` on EMNIST with the linear scaling rule, across 5 random trials. The mean accuracy is given in bold, with the standard deviation indicated by the pale region. We see that for $M = 200$, there are a number of catastrophic training failures, while for $M \geq 400$, all trials experienced catastrophic training failures.

accuracy) for EMNIST and Stack Overflow. Notably, while the training accuracy improvement also led to a test accuracy improvement for CIFAR-100, the same is not true for Shakespeare. In fact, the training benefits of the square root scaling there led to worse generalization across the board.

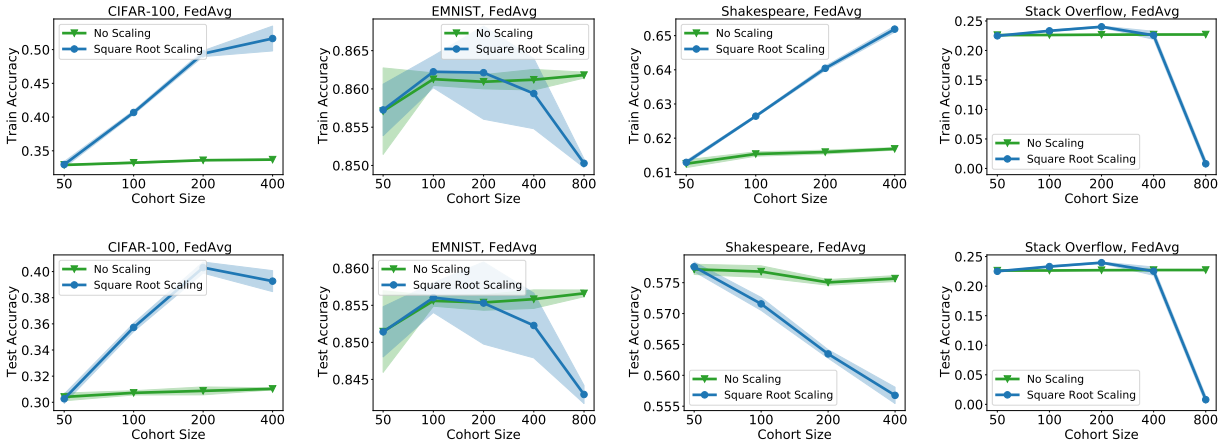

Figure 37. The train accuracy (top) and test accuracy (bottom) of `FedAvg` using square root scaling with warmup, versus no scaling, after training for 1500 communication rounds. Results are given for various cohort sizes and tasks

B.8. Dynamic Cohort Sizes

In this section, we plot the full results of using the dynamic cohort size strategy from Section 5. Recall that there, we use an analog of dynamic batch size methods for centralized learning, where the cohort size is increased over time. We specifically start with a cohort size of $M = 50$, and double every 300 communication rounds. If doubling would ever make the cohort size larger than the number of training clients, we simply use the full set of training clients in a cohort.

We plot the test accuracy of `FedAdam` and `FedAvg` using the dynamic cohort size, as well as fixed cohort sizes of $M = 50$ and $M = 400$ (for CIFAR-100 and Shakespeare) or $M = 800$. In Figure 38, the test accuracy is plotted with respect to the number of examples processed by the clients, in order to measure the data-efficiency of the various methods. We find that while the dynamic cohort strategy can help interpolate the data efficiency between small and large cohort sizes, obtaining the same data efficiency as $M = 50$ for most accuracy thresholds, then transitioning to the data efficiency of larger M.

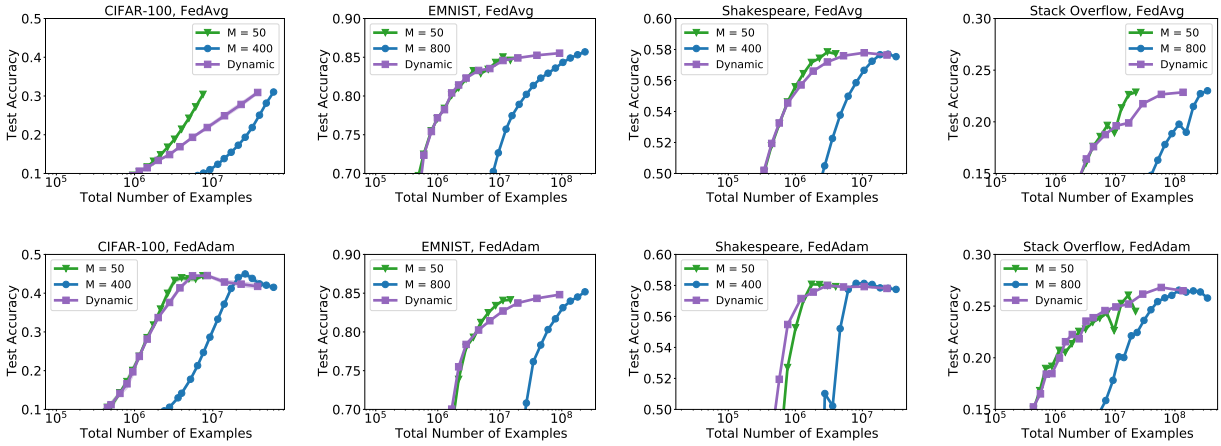

Figure 38. Test accuracy of `FedAvg` (top) and `FedAdam` (bottom) with respect to the total number of examples. Both algorithms are applied to various tasks, with various fixed cohort sizes, and the dynamically increasing cohort strategy.

In Figure 39, we plot the test accuracy of the methods discussed above with respect to the number of communication rounds, in order to better visualize the generalization behavior of the dynamic cohort strategy. We see that for `FedAvg`, there is little to no difference between the test accuracy for $M = 50$ and $M = 400$ or $M = 800$, and that the dynamic cohort strategy generally lays in-between these two. This is partially a consequence of the diminishing returns discussed in Section 3.2. For `FedAdam`, we see that there are more returns to be had for increasing the cohort size. Moreover, we see that the dynamic cohort strategy typically begins at the accuracy level of $M = 50$, and later matches that of the larger cohort. This can be beneficial such as in the case of Stack Overflow, or it can be detrimental as in the case of CIFAR-100, where we see that the dynamic cohort strategy faces the generalization issues in Section 3.3. Thus, we see that the dynamic cohort strategy can help improve the data efficiency of large cohort training, but cannot remedy issues of diminishing returns or generalization failures.

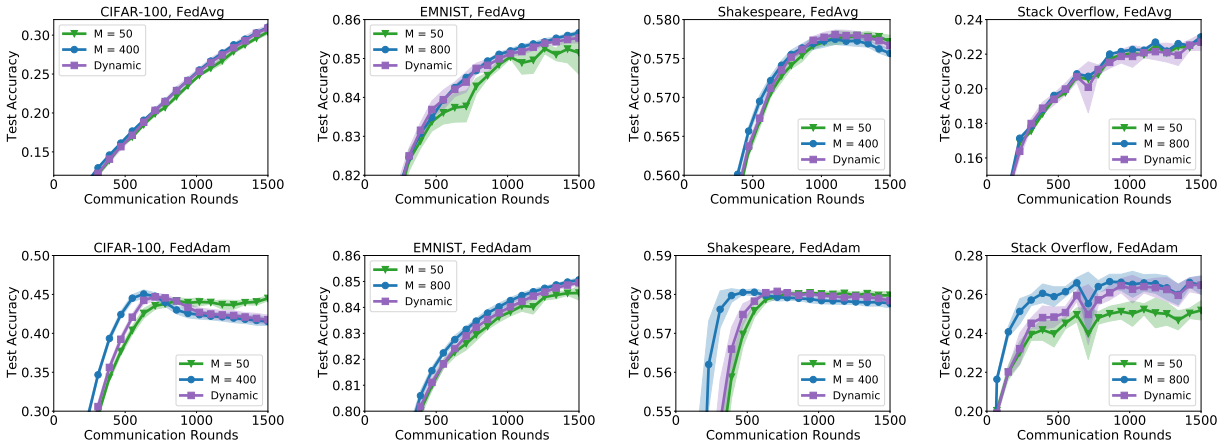

Figure 39. Test accuracy of `FedAvg` (top) and `FedAdam` (bottom) with respect to the total number of communication rounds. Both algorithms are applied to various tasks, with various fixed cohort sizes, and the dynamically increasing cohort strategy.

B.9. Changing the Number of Local Steps

While the cohort size has clear parallels to batch size, it is not the only factor determining the number of examples seen per round in Algorithm 1. The number of client epochs E and the client batch size also affect this. To study this "effective batch size" in FL, we fix the client batch size, and investigate how the cohort size and number of local steps simultaneously impact the performance of `FedAvg`.

In particular, we fix a local batch size of 1 and vary the cohort size over $\{16, 32, \ldots, 1024\}$. We vary the number of local steps over $\{1, 2, 4, \ldots, 256\}$. We plot the number of rounds needed for convergence, and the final test accuracy in Figure 40. By construction, each square on an anti-diagonal corresponds to the same number of examples per round.

In the left figure, we see that if we fix the cohort size, then increasing the number of local steps can accelerate convergence, but only up to a point, after which catastrophic training failures occur. By contrast, if we have convergence for some number of local steps and cohort size, convergence occurs for all cohort sizes. Similarly, we see in the right hand figure that increasing the number of local steps can drastically reduce generalization, more so than increasing the cohort size. In essence, we see that the number of local steps obeys many of the same issues outlined in Section 3. Therefore, correctly tuning the number of local steps in unison with the cohort size may be critical to ensuring good performance of large-cohort methods.

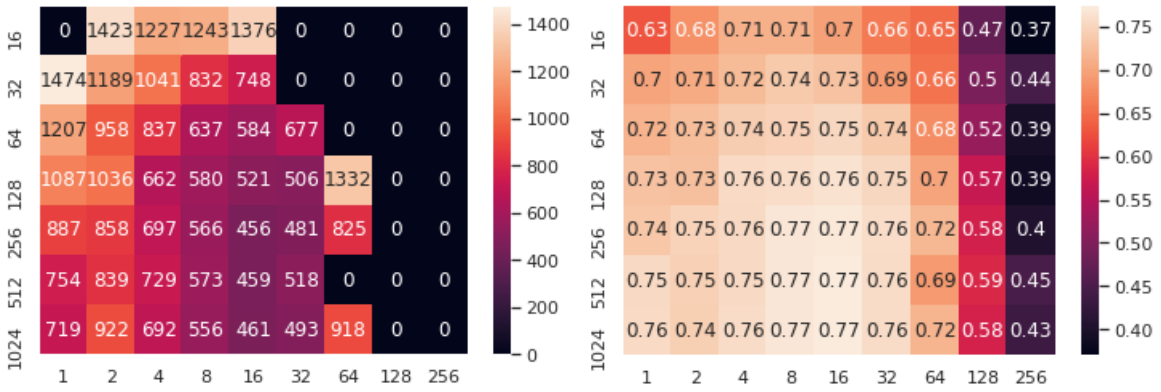

Figure 40. The number of rounds for to reach a test accuracy of 70% (left) and the test accuracy after 1500 rounds (right). Results are for `FedAvg` on EMNIST with varying numbers of local steps (x-axis) and cohort sizes (y-axis).

B.10. Normalized `FedAvg`

While the methods above show promise in resolving some of the issues of large-cohort training, they also introduce extra hyperparameters (such as what type of learning rate scaling to use, or how often to double the cohort size). Notably, hyperparameter tuning can be difficult in federated learning, especially cross-device federated learning (Kairouz et al., 2021). Even adaptive methods like `FedAdam` introduce a number of new hyperparameters that can be challenging to contend with. We are therefore motivated to design a large-cohort training method that does not introduce any new hyperparameters.

Recall that in Section 4, we showed that for `FedAvg`, the client updates (Δ_k^t in Algorithm 1 and Algorithm 2) are nearly orthogonal in expectation. By averaging nearly orthogonal updates in large-cohort training, we get a server pseudo-gradient Δ^t that is close to zero, meaning that the server does not make much progress at each communication round. In order to compensate for this without having to tune a learning rate scaling strategy, we propose a simple variant of `FedAvg` that tries to account for this near-orthogonality of client updates. Rather than applying SGD to the server pseudo-gradient (as in Algorithm 1), we apply SGD to the normalized server pseudo-gradient. That is, the server updates its model via

$$x' = x - \eta_s \frac{\Delta}{\|\Delta\|_2}.$$

This is a kind of federated analog of normalized SGD methods used for centralized learning (Nacson et al., 2019). It introduces no new hyperparameters with respect to Algorithm 1. To test this method, which we refer to as normalized `FedAvg`, we present its training and test accuracy versus cohort size in Figure 41. Notably, we do not re-tune any learning rates. We simply use the same learning rates tuned for (unnormalized) `FedAvg`.

We find that for most cohort sizes and on most tasks, normalized `FedAvg` achieves better training accuracy for larger cohorts. Thus, this helps mitigate the diminishing returns issue in Section 3.2. We note two important exceptions: for EMNIST, the normalized `FedAvg` is slightly worse for all cohort sizes. For Stack Overflow, it obtains worse training accuracy for the largest cohort size. However, we see significant improvements on CIFAR-100 and all but the largest cohort

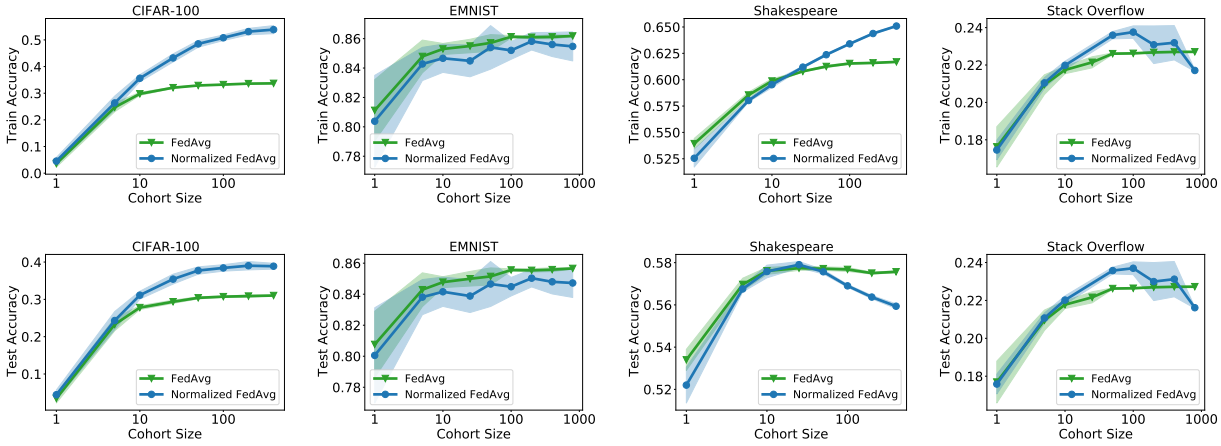

Figure 41. The train accuracy (top) and test accuracy (bottom) of `FedAvg` and the normalized variant of `FedAvg`, after training for 1500 communication rounds. Results are given for various cohort sizes and tasks

sizes for Stack Overflow. We believe that the method therefore exhibits promising results, and may be improved in future work.